

Effect of Gravitational Waves on Yang-Mills condensates

Narasimha Reddy Gosala^{*}, Arundhati Dasgupta[†]

4401 University Drive, Department of Physics and Astronomy,
University of Lethbridge, Canada.

Abstract

In this article, we investigate the interactions of a Yang-Mills (YM) wave fluctuation of a classical isotropic, homogeneous YM condensate, which models gluon plasma, with a Gravitational Wave (GW). We re-analyse the study of fluctuations of the gluon plasma using vector decomposition of the gauge field into scalar, longitudinal, and transverse modes. We find that there is an energy transfer between isotropic gluon condensate and plasmon modes, but the effect is delayed, and dependent on the initial conditions. We also studied quarks in the background of YM condensate and GW. We find that the quarks break the isotropy of the condensate and the GW couples quarks of different flavours of the SU(2) group. The GW induces flavour fluctuations, and this has interesting implications for experimental observations and quark-gluon plasma physics.

1 Introduction

Yang-Mills (YM) fields are known to play an important role in understanding the dynamics of varied phenomena in both early universe and relativistic heavy ion collisions. The non-perturbative YM fields play an important role in the study of quark confinement and chiral symmetry-breaking phenomena in Quantum Chromodynamics (QCD) [1–3]. The self-interacting non-abelian gauge fields help in understanding Quark-Gluon Plasma (QGP) [4–7] which is postulated to have formed in the early universe and also being observed in heavy-ion collisions. The classical YM fields help in the study of the non-equilibrium matter formed at early times in heavy-ion collisions before the formation of QGP [8, 9]. YM fields also play a significant part in the study of many aspects of cosmology like Dark Energy [10, 11] and gauge field-driven inflation [12, 13]. Also, they are expected to play an important role in understanding QCD vacuum energy [14–16].

QGP is a dense state of matter, primarily consisting of quarks and gluons in an unconfined state. Most of the studies relating to the study of QGP are based on its thermodynamic properties like using the Bag model [17]. There are some studies related to QCD phase transition, which led to the formation of QGP, based on effective field theories like the NJL model [18]. Some studies related to investigating QGP assume quarks and gluons propagate as waves owing to their unconfined state. Since there were many processes which generate gravitational waves (GWs) in the early universe [19–22], it is quite natural to expect an influence of GWs on QGP or in general cosmological processes. This motivates us to study the de-confined YM fields in the presence of GWs. Along these lines, we studied the interaction of GWs with progressive YM fields in different cosmological backgrounds in [23]. In this paper, we extend that analysis for a homogeneous and isotropic YM condensate configuration along with fluctuations in a GW background.

The study of QGP using condensate and fluctuations were carried out by several authors [24–29]. Using effective action analysis, it is found that the true vacuum state of YM theory can be described by a nonzero chromomagnetic gluon condensate [30]. Considering the YM ground state as a condensate and studying the

^{*}narasimha.gosala@uleth.ca

[†]arundhati.dasgupta@uleth.ca

fluctuations around this ground state will give a better understanding of QGP. Along these lines, Prokhorov, Pasechnik, and Vereshkov [24] have studied the dynamics of fluctuations in the presence of SU(2) YM condensate. In their work, they consider a spatially homogeneous and isotropic component of gauge field as a condensate and an inhomogeneous component as YM wave modes. It was shown that the interactions between large condensate and small YM modes set off a significant energy transfer from condensate to wave modes. They found that the longitudinal YM modes which are un-physical in degenerate YM theory become physical particles, acquiring frequency and dispersion, after quantization due to the interactions between condensate and wave modes. Later, the authors studied YM condensates [28] in the SU(3) case which has 3 SU(2) subgroups, giving rise to interaction among 3 different overlapping SU(2) condensates. We found this model of the YM condensate to be most useful to study the interactions with GW. This model of the plasma and the plasmons allowed us to extend the work of [23] which studies the interaction of GW with YM progressive waves to the study of the interaction of a GW with a YM plasma-plasmon system. We label the condensate as the ‘plasma’ and the other modes as the plasmons (or particles).

There have been studies on the generation of GWs from QCD phase transition by considering the phase transition as a first-order phase transition [19] while some considered a different process from the relaxation of gluon condensate during QCD phase transition [31]. In this paper, we analyse the condensate of [24] in the presence of a GW. Our aim was to study how a GW can generate a plasmon fluctuation on the YM plasma. We find that symmetric transverse modes identified in [24] are induced by the GW, but the longitudinal modes are not induced to first order in the fields. To identify the longitudinal and transverse modes of the propagating vector fluctuations in a transparent way, we consider an ansatz which is different than in [24]. In this new ansatz, the condensate is taken as a homogeneous and isotropic solution of the SU(2) YM, as in [24], and a singlet under SU(2) transformations. However, the other vector modes are isolated as (Φ^a) longitudinal modes and transverse ones (χ_σ^a) , where $\sigma = 1, 2$, and $a = 1, 2, 3$ are the internal directions. We then analyze the system using similar methods as [24] and find that the energy exchange of the condensate with the other modes is delayed in time compared to [24]. We also find that after some time, the energy oscillates between the condensate and the plasmons, and subsequently the analysis breaks down as the non-perturbative self-interaction of the non-Abelian gauge field sets in. Note in most of our calculations, we use exact solutions to the system and do not use linearized approximations as in [24].

Then, we studied the condensate + fluctuations system in the presence of GWs. We find that the GW can perturb the condensate and induce the ‘plasmon modes’ or ‘particles’ which carry away the energy. We also analyzed the system perturbatively and numerical solutions were obtained. The GW interacts with the longitudinal modes as well as the transverse modes. In the presence of GW, the plasmon oscillations were generated even when they were zero initially. This can be understood as the GW initiating condensate decay into plasmons. These GW wave-induced ‘plasmons’ are obtained using both the longitudinal and transverse modes of the YM gauge fields.

Since QGP has quarks, we studied the combined system of condensate and massless Fermions. There were many studies on the Fermions in the background of gauge fields during different scenarios [32–36]. The previous works in this area have focused on massless Fermions [32] and also on the production and back reaction of massive Fermions in spontaneously broken gauge theory [33, 34] and during axion inflation [35, 36]. In this work, we consider the massless Fermions in the background of an SU(2) YM condensate. We find that Fermions break the isotropy and homogeneity assumption of the condensate upon back-reaction.

Further, we studied the condensate + Fermions system in the presence of GWs. We find that the GW coupled to the quark-condensate system induces flavour fluctuations. This is an interesting aspect of the calculations, which will have consequences for the quantum theory of QGP. We are working on further understanding the system [37]. In previous work [38], there has been an attempt to attribute the low viscosity of the QGP to gravitons. Our calculations suggest that the GW background might shed light on this when one computes the QGP thermodynamics. In [39], the graviton-induced flavour transitions have been studied and form factors obtained. In our calculations, the gravitational interaction is a classical wave, which is

appropriate for the energies of the QGP production in RHIC. However, we expect new results, when we use the new flavour-inducing transitions in the strangeness enhancement calculations of [40, 41]. QGP phase in heavy ion collisions is known to lead to strange flavour heavy quark generation. Our GW interaction terms will add to the strangeness generation form factors [40, 41].

The paper is organized as follows: in Sec. 2, we describe the condensate model of [24], their linearized analysis, and show how a GW interacts with it. In Sec. 3, we re-analyze the condensate system using a varied decomposition and use non-perturbative analysis. In Sec. 4, we add Fermions to the system and describe how the quarks interact with the condensate and the GW. Finally, we conclude in Sec. 5.

2 Fluctuations around Condensate in Linear-order approximation

Consider the SU(2) Yang-Mills (YM) theory with a gauge invariant Lagrangian [42]

$$\mathcal{L} = -\frac{1}{4}F^{a\mu\nu}F_{\mu\nu}^a, \quad (1)$$

where $F_{\mu\nu}^a$ is the anti-symmetric field strength tensor of gauge field A_μ^a given by

$$F_{\mu\nu}^a = \partial_\mu A_\nu^a - \partial_\nu A_\mu^a + g_{\text{ym}}\varepsilon^{abc}A_\mu^b A_\nu^c, \quad (2)$$

where g_{ym} is the YM coupling constant and $F_{\mu\nu} = F_{\mu\nu}^a T^a$, with the generators T^a of Lie algebra, indexed by a , satisfying $\text{Tr}(T^a T^b) = \frac{1}{2}\delta^{ab}$, $[T^a, T^b] = i\varepsilon^{abc}T^c$ here ε^{abc} are the structure constants of Lie algebra. Greek indices represent the space-time coordinates and Latin indices represent the internal indices of the gauge group, for a SU(N) group, one has $a, b, c = 1, \dots, N^2 - 1$.

The equations of motion corresponding to the above Lagrangian are

$$\nabla_\mu F^{a\mu\nu} + g_{\text{ym}}\varepsilon^{abc}A_\mu^b F^{c\mu\nu} = 0, \quad (3)$$

where ∇_μ is the covariant derivative. As suggested in [43–46], the SU(2) YM field can be represented in terms of a homogeneous isotropic configuration parametrized by a single scalar function due to the isomorphism of SU(2) group and the SO(3) group of spatial rotations. From here on, we consider the Latin indices for both internal indices of SU(2) and for space indices. As in the work of [24], we considered the following ansatz in the Hamilton gauge, $A_0^a = 0$,

$$A_i^a = U(t)\delta_i^a + \delta^{ak}\tilde{A}_{ki}(t, \vec{x}), \quad (4)$$

where $U(t)$ is the spatially homogeneous time-dependent scalar field corresponding to the YM condensate and \tilde{A}_{ik} is the spatially in-homogeneous fluctuations component. When the fluctuations are set to zero, the YM equation (3) reduces to

$$\partial_0\partial_0 U + 2g_{\text{ym}}^2 U^3 = 0. \quad (5)$$

The exact solution for the above equation is given in terms of Jacobi elliptic functions as

$$U(t) = c_1 \text{sn}(g_{\text{ym}}c_1(t+c_2), -1), \quad (6)$$

where $\text{sn}(g_{\text{ym}}c_1(t+c_2), -1)$ is the sine Jacobi elliptic function and c_1 and c_2 are the constants of integration (We used the notation $\text{sn}(u, k^2)$, where k is the elliptic modulus). Now, consider the linear order approximation in which only the interaction between condensate and fluctuations was taken into account. The YM equations were given by

$$\square\tilde{A}_{nk} - \partial_i\partial_k\tilde{A}_{ni} + g_{\text{ym}}U(2\varepsilon_{nic}\partial_i\tilde{A}_{ck} + \varepsilon_{nbk}\partial_i\tilde{A}_{bi} + \varepsilon_{nbc}\partial_k\tilde{A}_{bc}) + g_{\text{ym}}^2 U^2(\tilde{A}_{kn} - \tilde{A}_{nk} - 2\tilde{A}_{ii}\delta_{nk}) = 0. \quad (7)$$

The constraint equation (Gauss's Constraint) in the linearized form is given by

$$\partial_i \partial_0 \tilde{A}_{ni} + g_{ym} \partial_0 U \varepsilon_{nki} \tilde{A}_{ki} + g_{ym} U \varepsilon_{nik} \partial_0 \tilde{A}_{ki} = 0. \quad (8)$$

In [24], the fluctuations \tilde{A}_{ki} are decomposed into longitudinal and transverse modes. However, in the following, we analyze the symmetric transverse trace-less modes only, as the GW interacts with only these. The GW doesn't couple to the longitudinal modes in this particular analysis. The trace-less modes of the fluctuations are

$$\tilde{A}_{ik} = Q_{ik}^\alpha \Psi_\alpha, \quad (9)$$

where the coefficient Q_{ik}^α satisfies the following conditions: $Q_{ik}^\alpha = Q_{ki}^\alpha$, $Q_{ii}^\alpha = 0$ and α take the values 1 and 2. If the YM fluctuation mode is propagating in the z -direction, then the only non-zero components of Q_{ik}^α are $Q_{11}^1 = -Q_{22}^1 = 1$ and $Q_{12}^2 = Q_{21}^2 = 1$. With this choice of modes, the constraint equation gets automatically satisfied and the equations for the modes Ψ_α are given by

$$\square \Psi_1 - 2g_{ym} U \partial_z \Psi_2 = 0, \quad (10)$$

$$\square \Psi_2 + 2g_{ym} U \partial_z \Psi_1 = 0. \quad (11)$$

In Fourier space, these equations can be written as generalized Mathieu equations. These equations were well studied in the case of parametric resonance [47–49].

We solved the above equations using Mathematica using the Method of Lines, a numerical technique to solve PDEs (see Appendix A). The numerical solutions for Ψ_α are shown in Figs. (1a) & (1b).

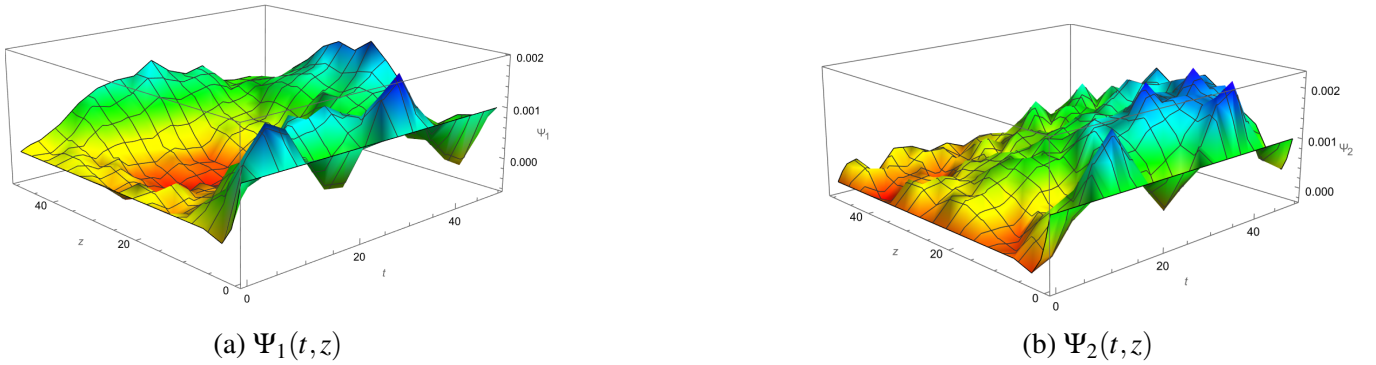


Figure 1: Figures showing $\Psi_1(t, z)$ and $\Psi_2(t, z)$ in the presence of a condensate. We choose $g_{ym} = 0.5$, $c_1 = c_2 = 1$, $\Psi_1(0, z) = \Psi_2(0, z) = 0.001$ and $\Psi_1(t, 0) = \Psi_2(t, 0) = 0$.

Without the Fourier transform as in [24], we obtained solutions for the transverse modes and show that the $\Psi_2(t, z)$ decreases with z as in Fig. (1b). However $\Psi_1(t, z)$ has a different behavior, with a trough at $z = 20$ in Fig. (1a). These numerical solutions show that transverse modes are induced by the condensate. However, these fields have to be non-zero at $t = 0$ for them to evolve. The question we ask is if GW can induce these modes from the condensate at $t = 0$. The above would correspond to the system of fluctuations studied in [24], with only the Ψ_α , with non-zero initial boundary conditions. We study a simplified version of [24], as the GW only couples or interacts with the symmetric transverse tensor modes of \tilde{A}_{ik} . This is expected due to the nature of the GW which is a symmetric transverse tensor.

2.1 In the presence of Gravitational waves

In this subsection, we want to study the fluctuations around a condensate in the presence of a GW. Here, we start with the YM equations in a general metric as in [23]

$$\frac{1}{\sqrt{-g}} \partial_\mu \left(\sqrt{-g} g^{\mu\lambda} g^{\nu\rho} F_{\lambda\rho}^a \right) + g_{ym} \varepsilon^{abc} A_\mu^b F^{\mu\nu c} = 0. \quad (12)$$

In the linearized approximation, using the GW metric i.e. $g_{\mu\nu} = \eta_{\mu\nu} + h_{\mu\nu}$, we can split the equation in the following form, where we have taken the GW wave-dependent terms to one side as follows

$$\eta^{\mu\lambda}\eta^{\nu\rho}\partial_\mu F_{\lambda\rho}^a + g_{\text{ym}}\varepsilon^{abc}A_\mu^b F^{\mu\nu c} = g_{\text{ym}}\varepsilon^{abc}A_\mu^b h^{\mu\lambda}\eta^{\nu\rho}F_{\lambda\rho}^c + g_{\text{ym}}\varepsilon^{abc}A_\mu^b h^{\nu\rho}\eta^{\mu\lambda}F_{\lambda\rho}^c + \eta^{\nu\rho}\partial_\mu F_{\lambda\rho}^a h^{\mu\lambda} + \eta^{\mu\lambda}\partial_\mu(h^{\nu\rho}F_{\lambda\rho}^a). \quad (13)$$

We then solve the above equations using the same form of ansatz as in the previous section. In Hamilton gauge $A_0^a = 0$, the ansatz is written as

$$A_i^a = U(t)\delta_i^a + \delta^{ak}\tilde{A}'_{ki}, \quad (14)$$

where \tilde{A}'_{ki} is the fluctuations component of the gauge field due to its interaction with condensate and gravitational wave which is different from \tilde{A}_{ki} of Eq. (4), whose dependence was on the condensate only. In linear-order approximation, the YM equation can be written as

$$\square\tilde{A}'_{nk} - \partial_i\partial_k\tilde{A}'_{ni} + g_{\text{ym}}U(2\varepsilon_{nic}\partial_i\tilde{A}'_{ck} + \varepsilon_{nbk}\partial_i\tilde{A}'_{bi} + \varepsilon_{nbc}\partial_k\tilde{A}'_{bc}) + g_{\text{ym}}^2U^2(\tilde{A}'_{kn} - \tilde{A}'_{nk} - 2\tilde{A}'_{ii}\delta_{nk}) = -\partial_0(Uh_{kn}) + g_{\text{ym}}U^2\varepsilon_{nil}\partial_i h_{kl} - g_{\text{ym}}^2U^3h_{kn}. \quad (15)$$

We consider a plus-polarised GW to be propagating in the z -direction i.e. $h_{ik} = e_{ik}^+h_+$, where e_{ik}^+ is the polarisation vector of the gravitational wave with two non-zero values, $e_{11}^+ = -e_{22}^+ = 1$ and $h_+(t, z) = A_+\cos(\omega_g(t-z))$. Similarly, we consider only the same modes as in the previous section i.e. $\tilde{A}'_{ik} = Q_{ik}^\alpha\Psi'_\alpha$. Then, the YM equation reduces to

$$\square\Psi'_1 - 2g_{\text{ym}}U\partial_z\Psi'_2 = A_+(g_{\text{ym}}^2U^3\cos(\omega_g(t-z)) + \partial_0U A_+\omega_g\sin(\omega_g(t-z))), \quad (16)$$

$$\square\Psi'_2 + 2g_{\text{ym}}U\partial_z\Psi'_1 = -A_+g_{\text{ym}}\omega_gU^2\sin(\omega_g(t-z)). \quad (17)$$

We can solve the above equations using Mathematica and the numerical solutions are shown in Figs. (2a) & (2b).

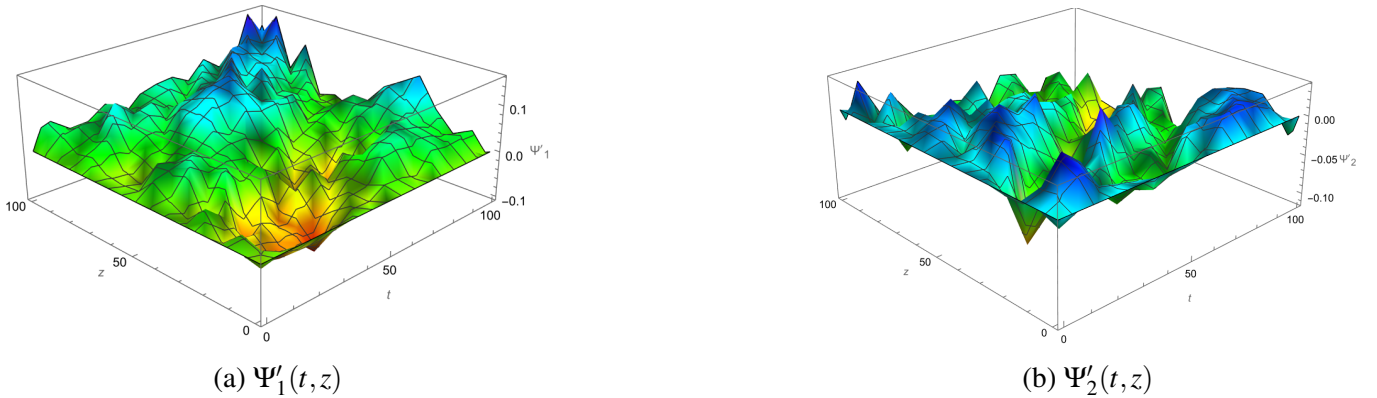


Figure 2: Figures showing $\Psi'_1(t, z)$ and $\Psi'_2(t, z)$ in the presence of a gravitational wave. We choose $g_{\text{ym}} = 0.5$, $c_1 = c_2 = 1$, $A_+ = 0.0001$ and $\omega_g = 100$.

Apart from the numerical solutions, we can also find the analytical solution by using the triad formalism. For this purpose, the gauge field can be rewritten using triads in the form of given in [24],

$$A_i^a = U(t)e_i^a + e^{ak}\tilde{A}_{ki}, \quad (18)$$

where e_i^a are soldering forms that connect the space-time metric to the SU(2) group manifold which satisfies the following conditions:

$$e_i^a e_{ak} = g_{ik}; \quad e_i^a e_b^i = \delta_b^a. \quad (19)$$

From the previous work [50], we take the triads in the case of a plus-polarised GW, to be

$$e_1^a = \left(\sqrt{(1+h_+(t,z))}, 0, 0 \right), \quad (20a)$$

$$e_2^a = \left(0, \sqrt{(1-h_+(t,z))}, 0 \right), \quad (20b)$$

$$e_3^a = (0, 0, 1). \quad (20c)$$

Taking the linear order approximation of triads, we can write the gauge field (Eq. (18)) as

$$A_i^a = U(t) \delta_i^a + \frac{1}{2} h_i^a U + \tilde{A}_i^a. \quad (21)$$

If we compare the above equation with Eq. (14), we find that the gauge field fluctuation in the presence of GW is related to the fluctuation without GW as

$$\tilde{A}'_i{}^a = \frac{1}{2} h_i^a U + \tilde{A}_i^a. \quad (22)$$

One can check that this solution indeed satisfies Eq. (15). In terms of Ψ_α and Ψ'_α , we found that

$$\Psi'_\alpha = \Psi_\alpha + \frac{1}{4} Q_{ik}^\alpha h_{ik} U. \quad (23)$$

In explicit forms, we get

$$\Psi'_1 = \Psi_1 + \frac{1}{2} h_+ U; \quad \Psi'_2 = \Psi_2. \quad (24)$$

In this simple analysis, we found an exact analytical solution for the fluctuation of the gauge field in the presence of both condensate and gravitational waves. One can see that even if at $t = 0$ the Ψ_1, Ψ_2 are zero, there is a Ψ'_1 induced due to the GW and the condensate interaction as in Eq. (24).

2.2 Higher order corrections

If one wants to work beyond linear order approximation as in [24], then one has to consider the interactions between the modes. Taking into account higher-order terms, the equations for Ψ_1 and Ψ_2 (Eqs. 10 & 11) changed to

$$\square \Psi_1 - 2g_{\text{ym}} U \partial_z \Psi_2 - g_{\text{ym}}^2 (\Psi_1^3 + \Psi_1 \Psi_2^2) = 0, \quad (25)$$

$$\square \Psi_2 + 2g_{\text{ym}} U \partial_z \Psi_1 - g_{\text{ym}}^2 (\Psi_2^3 + \Psi_1^2 \Psi_2) = 0. \quad (26)$$

The solutions for the above equations are given in Fig. (3). Similarly, in the case of GW, the Eqs. (16) & (17) changed to

$$\square \Psi'_1 - 2g_{\text{ym}} U \partial_z \Psi'_2 - g_{\text{ym}}^2 (\Psi_1'^3 + \Psi_1' \Psi_2'^2) = A_+ (g_{\text{ym}}^2 U^3 \cos(\omega_g(t-z)) + \partial_0 U A_+ \omega_g \sin(\omega_g(t-z))), \quad (27)$$

$$\square \Psi'_2 + 2g_{\text{ym}} U \partial_z \Psi'_1 - g_{\text{ym}}^2 (\Psi_2'^3 + \Psi_1'^2 \Psi_2') = -A_+ g_{\text{ym}} \omega_g U^2 \sin(\omega_g(t-z)). \quad (28)$$

The numerical solutions for the above equations are shown in Fig. (4). It is very hard to find the analytical solutions for these equations as opposed to the case in the previous section.

We have found that the transverse modes behave differently to the second order in the interactions, with GW. We also observe that a GW interacting with the condensate naturally induces the transverse modes. Thus we are ready to answer the energetics question, can GW induce a decay of the YM condensate? In the next section, we try a different ansatz and obtain a non-perturbative analysis of the ‘particles’ and then analyze the energy of the system.

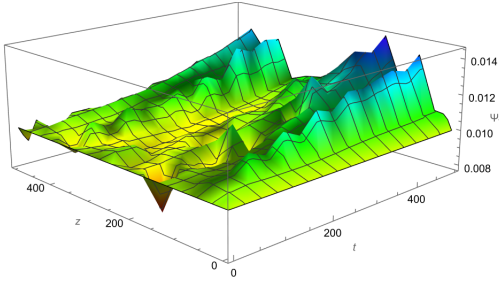
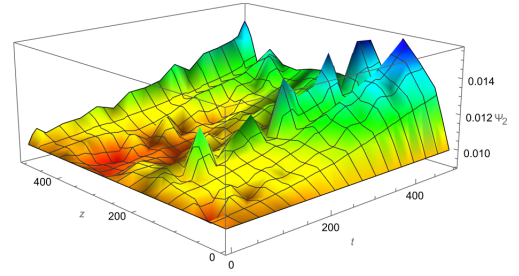
(a) $\Psi_1(t, z)$ (b) $\Psi_2(t, z)$

Figure 3: Figures showing $\Psi_1(t, z)$ and $\Psi_2(t, z)$ in the presence of condensate to second order in the self-interactions. We choose $g_{\text{ym}} = 0.5$ and $c_1 = c_2 = 1$.

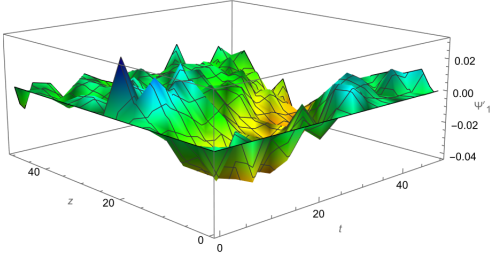
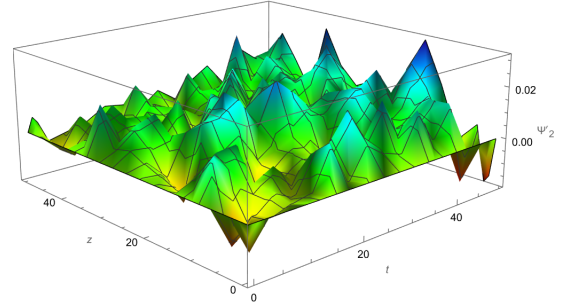
(a) $\Psi'_1(t, z)$ (b) $\Psi'_2(t, z)$

Figure 4: Figures showing $\Psi'_1(t, z)$ and $\Psi'_2(t, z)$ in the presence of a gravitational wave and condensate to second order in the self-interactions. We choose $g_{\text{ym}} = 0.5$, $c_1 = c_2 = 1$, $A_+ = 0.0001$ and $\omega_g = 50$.

2.3 Summary:

As is evident from the above, the GW changes the nature of the fluctuations over a YM condensate introduced in [24]. In particular, the transverse modes can be induced, even if the boundary conditions are set to zero for the transverse perturbations. The in-homogeneous terms in the Eqs. (27 & 28), are non-zero at $t = 0$, and or $z = 0$. This gives rise to non-zero solutions of Ψ'_1, Ψ'_2 , even if $\Psi'_{1(2)}(0) = 0$. This illustrates that a GW can induce these ‘plasmon’ modes from the condensate. This should then cause the condensate to lose energy into the ‘particles’ as in [24]. The longitudinal modes of the analysis of [24] do not see the GW. However, we try to analyse this split into transverse longitudinal vector modes in a more transparent way in the following section to analyze the energetics.

3 Vector Decomposition of YM Gauge Field

In this section, we discuss a different decomposition of the YM vector than what is used in [24]. This is motivated by [24], but we have a vector fluctuation of the condensate. This discussion avoids the use of the triads, and provides an independent analysis of the YM condensate, though very much in spirit to [24]. This avoids the use of the triads which is useful to introduce gauge-invariant fluctuations, but not to identify the longitudinal and transverse vector modes of the YM gauge field. We use the following decomposition

$$A_i^a(t, \vec{x}) = U(t)\delta_i^a + n_i\Phi^a(t, \vec{x}) + \varepsilon_{ijk}n_js_k^\sigma\chi_\sigma^a(t, \vec{x}). \quad (29)$$

Here, we have assumed, using the vector decomposition that it has longitudinal modes Φ^a for a vector propagating in the direction n_i . These are three, in number, in principle, but we set $n \cdot \Phi = 0$, which makes the number of independent components as 2. The χ_σ^a represents the transverse modes in the vector direction

s_i^σ where $\sigma = 1, 2$ represents the two transverse vectors to n_i and these are six in number. However, we impose the restriction that $(\vec{n} \times \vec{s}) \cdot \chi = 0$. Note the $U(t)$ cannot be classified as a longitudinal or transverse component. It is the Trace of the Gauge field $A_i^i = 3U(t)$. The Gauge condition is still Hamilton's gauge, with the $A_0^a = 0$. As the Lagrangian is independent of any space derivative for Φ^a , we assume it is only dependent on t . We also impose another restriction, in the internal directions. This restriction ensures that the form of the equations, the Kinetic terms of the three identified type of fields are de-coupled, and do not have any cross-terms. We assume $n \cdot \chi_\sigma = 0$ which is agreeable with the idea of removing the χ fields contribution in the soldered space along the longitudinal direction. This reduces another two degrees of freedom. The total degrees of freedom are therefore $1+2+3=6$. Thus requiring an isotropic 'independent' condensate reduces the number of degrees of freedom of the YM vector from 9 to 6. Now, of the above conditions, the first two are required to decouple the $U(t)$ kinetic terms from the plasmon modes. This is an important observation, as an isotropic and homogeneous condensate cannot be naturally obtained as dynamically decoupled from the gauge fields unless some additional conditions are imposed. This in particular the same as the [24] assumption of the gluon Heisenberg state. Next, considering the YM wave propagates in the z-direction i.e. $n = (0, 0, 1)$; $s^1 = (1, 0, 0)$, $s^2 = (0, 1, 0)$ and taking $\chi_1^2 = \chi_2^1 = 0$, we derived the equations of motion for $U(t)$, Φ^1, Φ^2 , $\chi_1^1 = \chi_1$ and $\chi_2^2 = \chi_2$. The details regarding the derivation of equations of motion is given in Appendix B.

$$\partial_0^2 U - \frac{2g_{ym}}{3} U \partial_z (\chi_1 + \chi_2) + g_{ym}^2 \left[2U^3 + \frac{1}{3} U ((\Phi^1)^2 + (\Phi^2)^2) + \frac{1}{3} U (\chi_1 + \chi_2)^2 - \frac{1}{3} (\chi_1 - \chi_2) \Phi_1 \Phi_2 \right] = 0, \quad (30)$$

$$\partial_0^2 \Phi^1 + g_{ym}^2 \left[U^2 \Phi^1 - U (\chi_1 - \chi_2) \Phi^2 + \Phi^1 \chi_2^2 \right] = 0, \quad (31)$$

$$\partial_0^2 \Phi^2 + g_{ym}^2 \left[U^2 \Phi^2 - U (\chi_1 - \chi_2) \Phi^1 + \Phi^2 \chi_1^2 \right] = 0, \quad (32)$$

$$\square \chi_1 + g_{ym}^2 \left[U \Phi^1 \Phi^2 - U^2 (\chi_1 + \chi_2) - \chi_1 \chi_2^2 - (\Phi^2)^2 \chi_1 \right] = 0, \quad (33)$$

$$\square \chi_2 - g_{ym}^2 \left[U \Phi^1 \Phi^2 + U^2 (\chi_1 + \chi_2) + \chi_1^2 \chi_2 + (\Phi^1)^2 \chi_2 \right] = 0. \quad (34)$$

We have also set some terms to zero which are of the form $\vec{n} \times \vec{\nabla} \chi_\sigma^a = 0$. This follows from the fact that the modes are propagating in the direction specified by \vec{n} . Note that the Gauss constraint is automatically satisfied when the above equations are solved for the $U(t), \Phi^1, \Phi^2, \chi_1, \chi_2$. As there are no derivatives in space for Φ^1, Φ^2 , we can take them to be dependent on time only without losing any dynamical information. All the space-dependent dynamics therefore is in the transverse modes, and we study that in the section with the GW. To facilitate a non-perturbative analysis of energy exchange we assume in the first approximation, that all the modes are independent of space, and are functions of time only. This allows us to describe the exchange of energy between the condensate and the longitudinal and transverse modes to all orders in a clean way.

We solved the above-coupled equations numerically using Mathematica. The time axis of the graphs was given in terms of the period of unperturbed condensate solution ($c_1 \text{sn}(g_{ym} c_1 (t + c_2), -1)$) which is $T_u = (4K(-1))/(g_{ym} U(0))$, where $K(-1)$ is the complete elliptic function. We find that the amplitude of condensate starts decreasing only after a certain time, and then instead of a monotonic decay, it increases again. This is shown in Fig. (5a). In the quantum scenario, this late perturbative decay of condensate is related to the vacuum expectation value of the condensate [51]. The time at which the decay of condensate

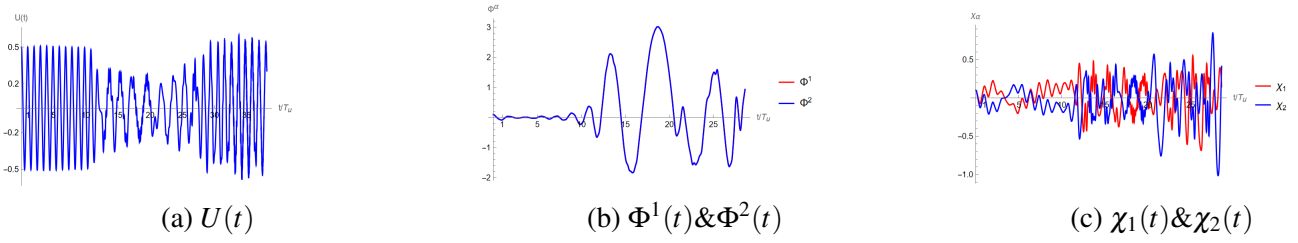


Figure 5: Figures showing $U, \Phi^1, \Phi^2, \chi_1$ and χ_2 as a function of time. We choose $g_{\text{ym}} = 0.5$, $U(0) = 0.5, \Phi^1(0) = 0.1, \Phi^2(0) = 0.1, \chi_1(0) = 0.1$ and $\chi_2(0) = 0.1$.

starts is defined as delay decay time (T_0). Also, one can see from Eqs. (31) & (32), the Φ^1 and Φ^2 have the same functional behavior and are also shown in Fig. (5b). The differential Eqs. (31, 32), are same except for the quadratic dependence in χ_1^2 and χ_2^2 , but these have same behaviour as discussed next. From Eqs. (33) & (34), the transverse modes differential equation differ from one another with signs which results in the almost complementary behavior of these functions as shown in Fig. (5c). From Fig. (5), we see that the longitudinal modes reach a very high magnitude as compared to the transverse modes for the same amount of time. This is again due to the quadratic nature of the potential terms in the Eqs. (31, 32).

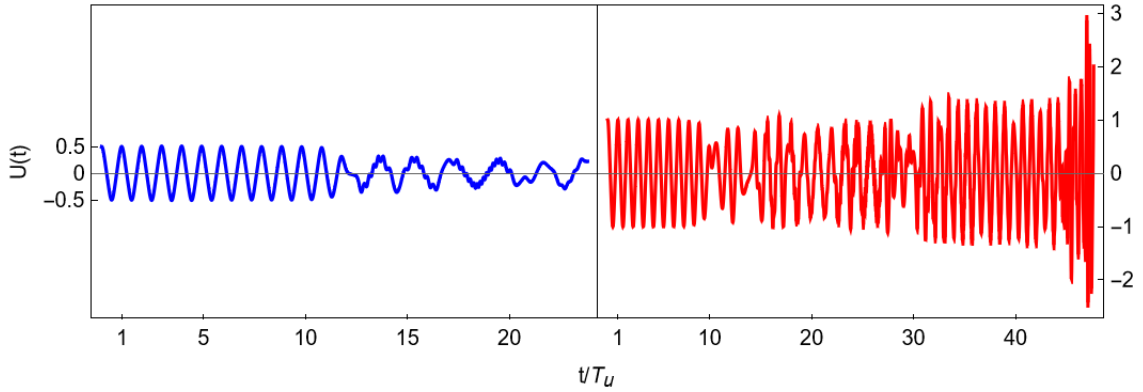


Figure 6: $U(t)$ for different initial conditions. The Blue plot corresponds to $U(0) = 0.5$ and the red plot corresponds to $U(0) = 1$ for the same $g = 0.5$ value. We choose $\Phi^1(0) = 0.1, \Phi^2(0) = 0.1, \chi_1(0) = 0.1$ and $\chi_2(0) = 0.1$.

If we change the initial value of condensate or coupling constant, we find that the point where the decreasing nature of the condensate happens also changes. This is shown in Figs. (6) & (7). We can observe that the decreasing behavior for different coupling constants and different initial conditions is happening around the same time. Since the Eqs. (33) & (34) are coupled, one can see that either one of the transverse modes will be generated even if the other mode is zero. Also, these Eqs. (33) & (34) contain a term ($g_{\text{ym}}^2 U \Phi^1 \Phi^2$) independent of transverse modes, this means we can generate the transverse modes even if they were zero initially as long as condensate and longitudinal modes are nonzero. From Eqs. (31 & 32), one can see that the longitudinal modes can be generated by the presence of the condensate $U(t)$ alone. This is a result of the self-interactions of the YM fields.

For the energy analysis, it is useful to construct the Hamiltonian density (\mathcal{H}) of the SU(2) YM system as a sum of contributions from condensate (\mathcal{H}_u), particles (\mathcal{H}_p) and the interaction term (\mathcal{H}_{int}) as follows

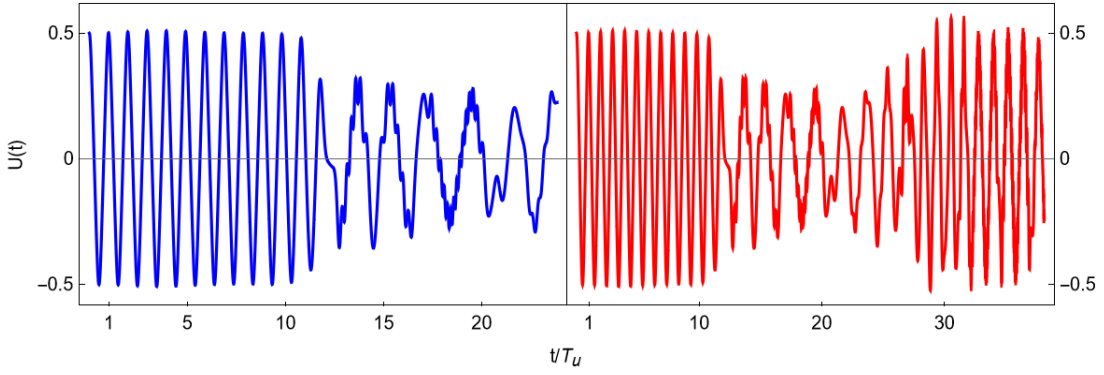


Figure 7: $U(t)$ for different g values. The Blue plot corresponds to $g = 0.5$ and the red plot corresponds to $g = 0.8$ for the same $U(0) = 0.5$ value. We choose $\Phi^1(0) = 0.1$, $\Phi^2(0) = 0.1$, $\chi_1(0) = 0.1$ and $\chi_2(0) = 0.1$.

$$\mathcal{H} = \mathcal{H}_u + \mathcal{H}_p + \mathcal{H}_{int}, \text{ where} \quad (35)$$

$$\mathcal{H}_u = \frac{3}{2}(\partial_t U \partial_t U + g_{ym}^2 U^4), \quad (36)$$

$$\mathcal{H}_p = \frac{1}{2}((\partial_t \Phi^1)^2 + (\partial_t \Phi^2)^2 + (\partial_t \chi_1)^2 + (\partial_t \chi_2)^2 + g_{ym}^2 \chi_1^2 \chi_2^2), \quad (37)$$

$$\mathcal{H}_{int} = \frac{1}{2}g_{ym}^2 [U^2((\Phi^1)^2 + (\Phi^2)^2 + \chi_1^2 + \chi_2^2) + (\Phi^1)^2 \chi_2^2 + (\Phi^2)^2 \chi_1^2 + 2U^2 \chi_1 \chi_2 - 2U \Phi^1 \Phi^2 (\chi_1 - \chi_2)]. \quad (38)$$

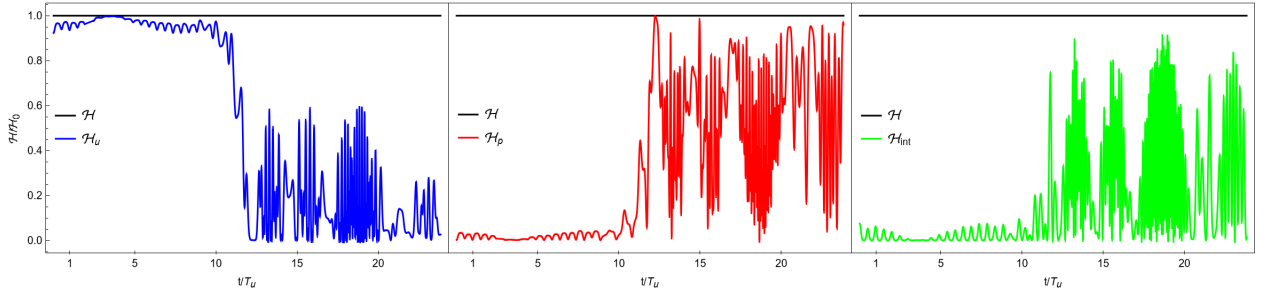


Figure 8: Figure showing the contributions of the condensate $\mathcal{H}_u(t)$, YM wave modes $\mathcal{H}_p(t)$ and interaction terms $\mathcal{H}_{int}(t)$ to the total energy $\mathcal{H}(t)$.

We see that the energy of the condensate (\mathcal{H}_u) is exchanged with the other modes (\mathcal{H}_p), but it is oscillatory. After T_0 time, we see that there is an energy swap effect between condensate and modes as predicted in [24]. This is shown in Fig.(8). We also found that the total energy of the system seems to increase after some time (Fig. 9). This indicates the breakdown of our ansatz: splitting the YM field into condensate, longitudinal, and transverse modes. After this time, there will be no isotropic and homogeneous condensate. Note our analysis is different from [24], as we have not assumed any space-dependence of the modes, as well as taken a different ansatz for the longitudinal and transverse modes decomposition. In our ansatz the ‘symmetry’ and ‘antisymmetric’ decomposition of the tensor modes of [24] is not required. The mode decomposition of [24] using the traids is gauge-invariant, which our decomposition is not. However the longitudinal and transverse ‘vector’ modes are identified, and the Hamiltonian, and the energy is gauge invariant, which is important.

3.1 In the presence of Gravitational Waves

Next, we study the above system in the presence of gravitational waves. Consider a gravitational wave propagating in the z -direction and assuming only one polarization, we can write the GW as $h_+(t, z) =$

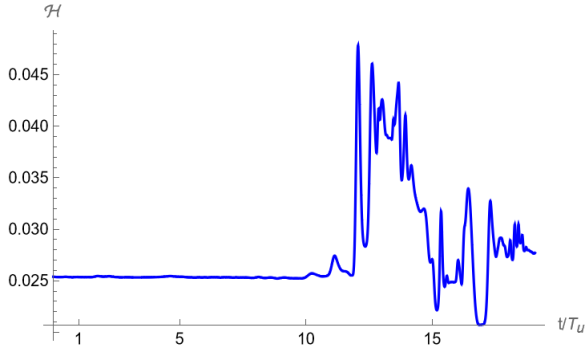


Figure 9: Figure showing the total energy $\mathcal{H}(t)$ as a function of time.

$A_+ \cos(\omega_g(t - z))$. Then, the equations of motion are as below:

$$\partial_0^2 U - \frac{2g_{ym}}{3} U (\partial_z(\chi_1 + \chi_2) + h_+ \partial_z(\chi_1 - \chi_2) + g_{ym}^2 [2U^3 + \frac{1}{3}U((\Phi^1)^2 + (\Phi^2)^2) + \frac{1}{3}U(\chi_1 + \chi_2)^2 - \frac{1}{3}(\chi_1 - \chi_2)\Phi^1\Phi^2]) - \frac{g_{ym}^2 h_+}{3} [U(\chi_2^2 - \chi_1^2 + (\Phi^2)^2 - (\Phi^1)^2) + \Phi^1\Phi^2(\chi_1 + \chi_2)] = 0, \quad (39)$$

$$\partial_0^2 \Phi^1 + g_{ym}^2 [U^2\Phi^1 - U(\chi_1 - \chi_2)\Phi^2 + \Phi^1\chi_2^2] - g_{ym}^2 h_+ [\chi_2^2\Phi^1 - U^2\Phi^1 + \Phi^2(\chi_1 + \chi_2)U] = 0, \quad (40)$$

$$\partial_0^2 \Phi^2 + g_{ym}^2 [U^2\Phi^2 - U(\chi_1 - \chi_2)\Phi^1 + \Phi^2\chi_1^2] - g_{ym}^2 h_+ [-\chi_1^2\Phi^2 + U^2\Phi^2 + \Phi^1(\chi_1 + \chi_2)U] = 0, \quad (41)$$

$$\square\chi_1 + h_+\square\chi_1 - \partial_t h_+ \partial_t \chi_1 + \partial_z h_+ \partial_z \chi_1 - g_{ym} U^2 \partial_z h_+ + g_{ym}^2 [U\Phi^1\Phi^2 - U^2(\chi_1 + \chi_2) - \chi_1\chi_2^2 + (\Phi^2)^2\chi_1] + g_{ym}^2 h_+ [-\chi_1(\Phi^2)^2 - U^2\chi_1 + \Phi^1\Phi^2 U] = 0, \quad (42)$$

$$\square\chi_2 - h_+\square\chi_2 + \partial_t h_+ \partial_t \chi_2 - \partial_z h_+ \partial_z \chi_2 + g_{ym} U^2 \partial_z h_+ - g_{ym}^2 [U\Phi^1\Phi^2 + U^2(\chi_1 + \chi_2) + \chi_1^2\chi_2 + (\Phi^1)^2\chi_2] + g_{ym}^2 h_+ [\chi_2(\Phi^1)^2 + U^2\chi_2 + \Phi^1\Phi^2 U] = 0. \quad (43)$$

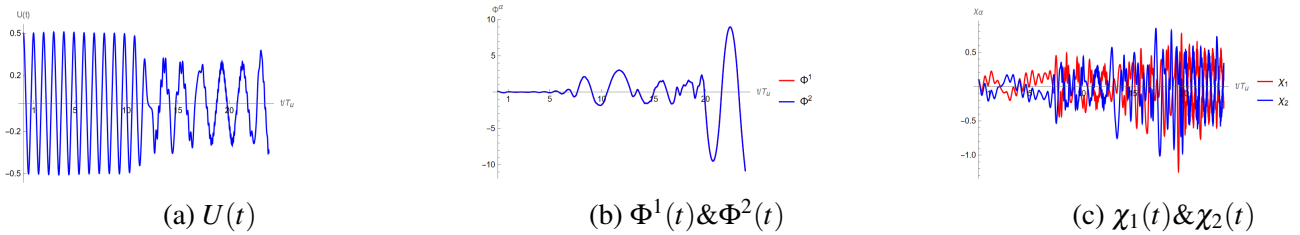


Figure 10: Figures showing $U, \Phi^1, \Phi^2, \chi_1$ and χ_2 as a function of time in the presence of a gravitational wave. We choose $g_{ym} = 0.5, U(0) = 0.5, A_+ = 0.001, \omega_g = 10, \Phi^1(0) = 0.1, \Phi^2(0) = 0.1, \chi_1(0) = 0.1$ and $\chi_2(0) = 0.1$.

To begin with, we set $z = 0$ and the equations are solved numerically using Mathematica considering the functions depend only on time, and plots are shown in Fig. (10). One can see from Fig. (11) that the solutions with GW approach the solutions without GW if the amplitude of GW (A_+) is much smaller than that of condensate and modes. We also find that if we take the GW amplitude (A_+) to be high, then the condensate solution is stable, even if the other modes are generated. From Eqs. (42) & (43), there is a term ($g_{ym} U^2 \partial_z h_+$) which does not depend on any wave modes. This shows that we can generate transverse modes even if they were zero initially. This makes sense if we think that the GW initiates the decay of the condensate.

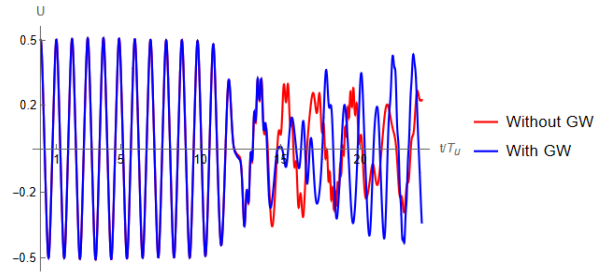


Figure 11: Figure showing $U(t)$ with and without GW cases. We choose $g_{\text{ym}} = 0.5$, $U(0) = 0.5$, $A_+ = 0.01$, $\omega_g = 10$, $\Phi^1(0) = 0.1$, $\Phi^2(0) = 0.1$, $\chi_1(0) = 0.1$ and $\chi_2(0) = 0.1$.



Figure 12: Figure showing energy density of condensate (\mathcal{H}_u) and particles/modes (\mathcal{H}_p) with and without GW cases. We choose $g_{\text{ym}} = 0.5$, $U(0) = 0.5$, $A_+ = 0.01$, $\omega_g = 10$, $\Phi^1(0) = 0.1$, $\Phi^2(0) = 0.1$, $\chi_1(0) = 0.1$ and $\chi_2(0) = 0.1$.

Similarly, we construct the Hamiltonian density (\mathcal{H}_{GW}) in the presence of GWs as follows

$$\mathcal{H}_{GW} = \mathcal{H}_{uGW} + \mathcal{H}_{pGW} + \mathcal{H}_{intGW}, \text{ where} \quad (44)$$

$$\mathcal{H}_{uGW} = \frac{3}{2}(\partial_t U \partial_t U + g_{\text{ym}}^2 U^4), \quad (45)$$

$$\mathcal{H}_{pGW} = \frac{1}{2}((\partial_t \Phi^1)^2 + (\partial_t \Phi^2)^2 + (\partial_t \chi_1)^2 + (\partial_t \chi_2)^2 + g_{\text{ym}}^2 \chi_1^2 \chi_2^2), \quad (46)$$

$$\begin{aligned} \mathcal{H}_{intGW} = & \frac{1}{2} g_{\text{ym}}^2 [U^2 ((\Phi^1)^2 + (\Phi^2)^2 + \chi_1^2 + \chi_2^2) + h_+ ((\Phi^1)^2 - (\Phi^2)^2 + \chi_1^2 - \chi_2^2) \\ & + (1 - h_+) (\Phi^1)^2 \chi_2^2 + (1 + h_+) (\Phi^2)^2 \chi_1^2 + 2U^2 \chi_1 \chi_2 \\ & - 2U \Phi^1 \Phi^2 ((1 + h_+) \chi_1 - (1 - h_+) \chi_2)] + \frac{1}{2} h_+ ((\partial_t \chi_1)^2 - (\partial_t \chi_2)^2). \end{aligned} \quad (47)$$

We also study the energy analysis of modes in the presence of GWs. Since the GWs have a very small magnitude, the effect of GWs on the wave modes energy is also very small. We obtained the same energy swap effect as in the previous section (Fig. (12)). If we take the GW amplitude to be high or comparable to that of condensate or modes, then GW stabilizes the condensate and the energy swap effect starts at much later times. This is shown in Fig. (13).

So far, we studied the system non-perturbatively by suppressing the z -dependence of the GW. To study the system with a z -dependence of the GW, we solve for the induced perturbations. We first assume there are no longitudinal modes ($\Phi^1 = \Phi^2 = 0$) and consider the reduced system (U, χ_1, χ_2). Note if we assume this without the GW, we find that there is no exchange of energy between condensate and χ modes. They are decoupled. There is an energy swap effect only when the longitudinal modes are non-zero. However, as we analyze, the GW can induce energy exchange without the longitudinal modes. Now consider a perturbation in YM field as $U(t) \rightarrow U(t) + \tilde{U}(t, z)$, $\chi_1(t) \rightarrow \chi_1(t) + \tilde{\chi}_1(t, z)$ and $\chi_2(t) \rightarrow \chi_2(t) + \tilde{\chi}_2(t, z)$. In the linear

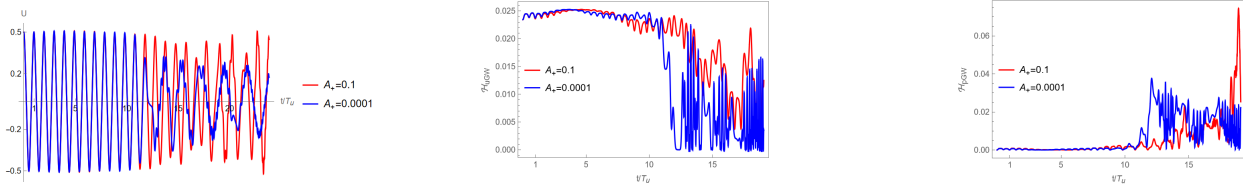


Figure 13: Figures showing condensate (first), the energy density of condensate (second), and the energy density of particles (third) as a function of time in the presence of a gravitational wave. We choose $g_{ym} = 0.5, \omega_g = 100, U(0) = 0.5, \Phi^1(0) = 0.1, \Phi^2(0) = 0.1, \chi_1(0) = 0.1$ and $\chi_2(0) = 0.1$.

order in h_+ and the perturbations, the equations become

$$\begin{aligned}
 -3\partial_t^2 \tilde{U} + 2\partial_z^2 \tilde{U} + 3g_{ym}U(\partial_z \tilde{\chi}_1 + \partial_z \tilde{\chi}_2) + g_{ym}^2 \left[\tilde{U}(-18U^2 - \chi_1^2 - \chi_2^2) - 2\tilde{U}\chi_1\chi_2 - 2U(\chi_1 + \chi_2)(\tilde{\chi}_1 + \tilde{\chi}_2) \right] \\
 -g_{ym}U(\chi_1 - \chi_2)\partial_z h_+ - g^2 h_+ U(\chi_2^2 - \chi_1^2) = 0, \tag{48}
 \end{aligned}$$

$$\begin{aligned}
 \square \tilde{\chi}_1 - 3g_{ym}U\partial_z \tilde{U} - g_{ym}^2 \left[U^2(\tilde{\chi}_1 + \tilde{\chi}_2) + 2U\tilde{U}(\chi_1 + \chi_2) + \tilde{\chi}_1\chi_2^2 + 2\chi_1\chi_2\tilde{\chi}_2 \right] \\
 -\partial_t \chi_1 \partial_t h_+ - h_+ \partial_t^2 \chi_1 - g_{ym}U^2 \partial_z h_+ - g_{ym}^2 h_+ U^2 \chi_1 = 0, \tag{49}
 \end{aligned}$$

$$\begin{aligned}
 \square \tilde{\chi}_2 - 3g_{ym}U\partial_z \tilde{U} - g_{ym}^2 \left[U^2(\tilde{\chi}_1 + \tilde{\chi}_2) + 2U\tilde{U}(\chi_1 + \chi_2) + \tilde{\chi}_2\chi_1^2 + 2\chi_1\chi_2\tilde{\chi}_1 \right] \\
 +\partial_t \chi_2 \partial_t h_+ + h_+ \partial_t^2 \chi_2 + g_{ym}U^2 \partial_z h_+ + g_{ym}^2 h_+ U^2 \chi_2 = 0. \tag{50}
 \end{aligned}$$

We solved the above equations using Mathematica and the numerical solutions were given in Fig. (14). We can see that the perturbation in U is very small during early times as agreeable with the exact solution (Fig. (10a)). We find that the condensate loses its homogeneity and isotropic nature and gets perturbed due to GW.

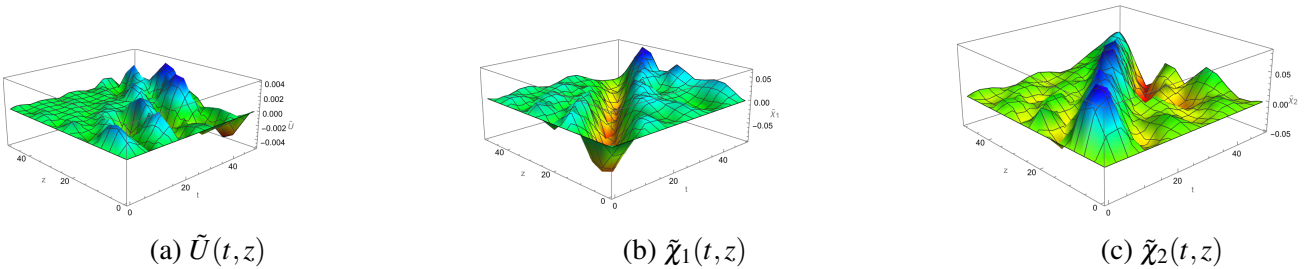


Figure 14: Figures showing $\tilde{U}(t, z), \tilde{\chi}_1(t, z)$ and $\tilde{\chi}_2(t, z)$ as a function of time and space in the presence of a gravitational wave. We choose $g_{ym} = 0.5, A_+ = 0.1$ and $\omega_g = 100$.

We also obtained the Hamiltonian density (\mathcal{H}) of the reduced system, up to second-order terms, as

follows

$$\mathcal{H} = \mathcal{H}' + \mathcal{H}'' + \mathcal{H}''', \text{ where} \quad (51)$$

$$\mathcal{H}' = \frac{3}{2} [(\partial_t U)^2 + g_{ym}^2 U^4] + \frac{1}{2} [(\partial_t \chi_1)^2 + (\partial_t \chi_2)^2 + g_{ym}^2 \chi_1^2 \chi_2^2] + \frac{1}{2} g_{ym}^2 U^2 (\chi_1 + \chi_2)^2, \quad (52)$$

$$\begin{aligned} \mathcal{H}'' = & 3\partial_t U \partial_t \tilde{U} + \partial_t \chi_1 \partial_t \tilde{\chi}_1 + \partial_t \chi_2 \partial_t \tilde{\chi}_2 + g_{ym} [2U \partial_z \tilde{U} (\chi_1 + \chi_2) - 2U^2 (\partial_z \tilde{\chi}_1 + \partial_z \tilde{\chi}_2)] \\ & + g_{ym}^2 [6U^3 \tilde{U} + U^2 (\chi_1 + \chi_2) (\tilde{\chi}_1 + \tilde{\chi}_2) + U \tilde{U} (\chi_1 + \chi_2)^2 + \chi_1 \chi_2^2 \tilde{\chi}_1] \\ & + \frac{1}{2} h_+ ((\partial_t \chi_1)^2 - (\partial_t \chi_2)^2) + \frac{1}{2} g_{ym}^2 h_+ U^2 (\chi_1^2 - \chi_2^2), \end{aligned} \quad (53)$$

$$\begin{aligned} \mathcal{H}''' = & \frac{3}{2} (\partial_t \tilde{U})^2 + (\partial_z \tilde{U})^2 + \frac{1}{2} [(\partial_t \tilde{\chi}_1)^2 + (\partial_z \tilde{\chi}_1)^2 + (\partial_t \tilde{\chi}_2)^2 + (\partial_z \tilde{\chi}_2)^2] + g_{ym} [\tilde{U} \partial_z \tilde{U} (\chi_1 + \chi_2) \\ & + U \partial_z \tilde{U} (\tilde{\chi}_1 + \tilde{\chi}_2) - 4U \tilde{U} (\partial_z \tilde{\chi}_1 + \partial_z \tilde{\chi}_2)] + \frac{1}{2} g_{ym}^2 [18U^2 \tilde{U}^2 + \tilde{U}^2 (\chi_1 + \chi_2)^2 + 4U \tilde{U} (\chi_1 + \chi_2) \\ & (\tilde{\chi}_1 + \tilde{\chi}_2) + U^2 (\tilde{\chi}_1 + \tilde{\chi}_2)^2 + \chi_1^2 \tilde{\chi}_2^2 + \chi_2^2 \tilde{\chi}_1^2 + 4\chi_1 \chi_2 \tilde{\chi}_1 \tilde{\chi}_2] + h_+ [\partial_t \chi_1 \partial_t \tilde{\chi}_1 + \partial_t \chi_1 \partial_t \tilde{\chi}_2] \\ & + g_{ym} h_+ (U \partial_z \tilde{U} (\chi_1 + \chi_2) - 2U^2 (\partial_z \tilde{\chi}_1 - \partial_z \tilde{\chi}_2)) + \frac{1}{2} g_{ym}^2 h_+ (2U \tilde{U} (\chi_1^2 - \chi_2^2) + 2U^2 (\chi_1 \tilde{\chi}_1 - \chi_2 \tilde{\chi}_2)). \end{aligned} \quad (54)$$

The perturbed energy plots are given in Figs. (15) & (16) as contributions from condensate and wave modes, respectively. These are the fluctuations over the zero-order energy density contribution of the condensate and modes, so they can be negative as shown in Fig. (16). As one can see the energy contribution due to GW is very small and there is an exchange of energy between condensate and particles but still oscillatory. If we keep the assumption that condensate as a homogeneous and isotropic configuration, then the equation for condensate will become a constraint on solutions of $\tilde{\chi}_1$ and $\tilde{\chi}_2$. Thus, we have to perturb the scalar mode with a z dependent function.

To verify that our perturbation theory works, we compare the solutions obtained Eqs. (49 & 50), with the ones obtained non-perturbatively. For comparison with the solutions of Eqs. (42, 43), we consider a reduced system (U, χ_1, χ_2) by taking only as functions of time (i.e. by solving the system at a particular z value ($z = 0$)). Then, we solved the reduced system $(U(t), \chi_1(t), \chi_2(t))$ in two ways: one is finding exact solution $(U_{GW}(t), \chi_{1GW}(t)$ and $\chi_{2GW}(t))$, and other is finding the perturbation solution $(\tilde{U}(t), \tilde{\chi}_1(t)$ and $\tilde{\chi}_2(t))$ by suppressing the z -dependence. We plot the solutions in Figs. (17). As one can see from Fig. (17a), the perturbation in U is very tiny and agrees with Fig. (14a). We can restore the longitudinal modes and compute the z dependence of the system with a GW, but the physics of the system has already been obtained here. Restoring the modes should not give any surprises.



Figure 15: Figures showing perturbed energy density contribution of condensate (left) and wave modes (right) as a function of time and space in the presence of a gravitational wave. We choose $g_{ym} = 0.5$, $A_+ = 0.1$ and $\omega_g = 10$.



Figure 16: Figures showing perturbed energy density contribution of condensate (Red plot) and wave modes (Blue plot) as a function of time and space separately in the presence of a gravitational wave. We choose $g_{ym} = 0.5$, $A_+ = 0.1$ and $\omega_g = 10$.

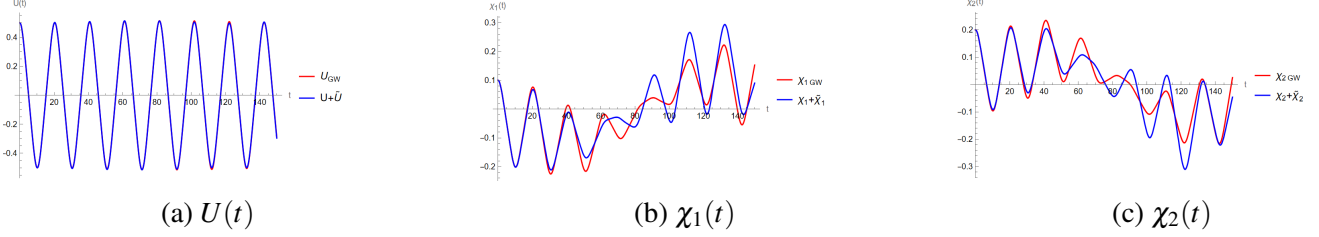


Figure 17: Figures showing $U(t)$, $\chi_1(t)$ and $\chi_2(t)$ as a function of time in the presence of a gravitational wave. We choose $g_{ym} = 0.5$, $A_+ = 0.1$, $\omega_g = 10$, $U(0) = 0.5$, $\chi_1(0) = 0.1$ and $\chi_2(0) = 0.2$.

3.2 Summary:

In this section, we have taken a vector decomposition of the SU(2) YM vector field. This is motivated by the decomposition of [24], but the ‘longitudinal’ and the ‘transverse’ modes are identified as a set of 2 & 6 component modes. The Energy exchange of the condensate with the modes is derived numerically, and we find that the ansatz breaks down after some time. This implies that our decomposition of the modes breaks down after some time due to the non-linear interactions. The separation of the energy into that of the condensate, the plasmons is not feasible after a delay. This is an important result and provides insight into how an isolated system of gluons might evolve. We find that a GW can induce the decay of the condensate into particles, but its effect is to delay the decay even further. Next, we discuss the same model by adding ‘quarks’ or Fermions to the condensate. Note, all our calculations are classical and we have not made a thermodynamic analysis of the system. However, thermodynamics is based on these fundamental interactions, and thus our study of the interactions can be used for a QGP analysis. Also our results are valid for SU(2) YM fields, but can be extended to SU(3) YM fields.

4 Interaction of Fermions in the presence of Condensate

In this section, we have a brief discussion of how YM condensate and Fermion fields might interact. The studies relating the Fermion production in the presence of SU(2) gauge fields were well studied in [52]. We take the SU(2) weak interactions, and a lepton doublet for the study to begin with. We take the YM condensate field as obtained in the previous discussion as the Jacobi elliptic function, and try to solve for the Fermion doublet in these backgrounds [53]. The Dirac equation for the Fermions is

$$i\gamma^\mu \partial_\mu \psi_\alpha + g_{ym} \gamma^\mu A_\mu^a T_{\alpha\beta}^a \psi_\beta = 0, \quad (55)$$

where T^a are the SU(2) generators, γ^μ are the four gamma matrices of the Clifford algebra and ψ_α are a SU(2) Fermion doublet with $\alpha = 1, 2$. Now as the condensate YM field is $A_i^a = U(t) \delta_i^a$, one solves for the Dirac equation in terms of this function. The solutions are analytically obtained in terms of Jacobi elliptic functions. We then study the back reaction of the Fermions on the condensate, in the spirit of [24]. Fermions

are not classical objects, and it makes sense only to study the bilinears built from them.

Taking the SU(2) generators to be $T^a = \sigma^a/2$, where σ^a are the Pauli matrices and labeling the Fermion doublets as (ψ_1, ψ_2) , the Dirac equation can be written as

$$i\gamma^\mu \partial_\mu \psi_1 + \frac{g_{ym}}{2} U(t) [(\gamma^1 - i\gamma^2) \psi_2 + \gamma^3 \psi_1] = 0, \quad (56)$$

$$i\gamma^\mu \partial_\mu \psi_2 + \frac{g_{ym}}{2} U(t) [(\gamma^1 + i\gamma^2) \psi_1 - \gamma^3 \psi_2] = 0. \quad (57)$$

We further solve these using the chiral representation of the gamma matrices for the Left and Right chirality Fermions as (ψ_{1L}, ψ_{1R}) and (ψ_{2L}, ψ_{2R}) , respectively. If the Fermions are quarks and the SU(2) group the isospin group, then the left quarks are a doublet, whereas the right quarks are singlets. However, here we assume that these are both doublets. Therefore, in principle, these can be a partial SU(3) system.

$$i(\partial_0 - \vec{\sigma} \cdot \vec{\partial}) \psi_{1L} - \frac{g_{ym}}{2} U(t) [(\sigma^1 - i\sigma^2) \psi_{2L} + \sigma^3 \psi_{1L}] = 0, \quad (58)$$

$$i(\partial_0 + \vec{\sigma} \cdot \vec{\partial}) \psi_{1R} + \frac{g_{ym}}{2} U(t) [(\sigma^1 - i\sigma^2) \psi_{2R} + \sigma^3 \psi_{1R}] = 0, \quad (59)$$

$$i(\partial_0 - \vec{\sigma} \cdot \vec{\partial}) \psi_{2L} - \frac{g_{ym}}{2} U(t) [(\sigma^1 + i\sigma^2) \psi_{1L} - \sigma^3 \psi_{2L}] = 0, \quad (60)$$

$$i(\partial_0 + \vec{\sigma} \cdot \vec{\partial}) \psi_{2R} + \frac{g_{ym}}{2} U(t) [(\sigma^1 + i\sigma^2) \psi_{1R} - \sigma^3 \psi_{2R}] = 0. \quad (61)$$

At the level of the two-component equations for the Weyl Fermions written as (ψ_{1L1}, ψ_{1L2}) and (ψ_{2L1}, ψ_{2L2}) , we keep only the Left-handed quarks which form a doublet, e.g. (u_L, d_L) , as non-zero. The equations are solved when the wave functions only depend on time:

$$i\partial_0 \psi_{1L1} - \frac{g_{ym}}{2} U(t) \psi_{1L1} = 0, \quad (62)$$

$$i\partial_0 \psi_{1L2} - g_{ym} U(t) \psi_{2L1} + \frac{g_{ym}}{2} U(t) \psi_{1L2} = 0, \quad (63)$$

$$i\partial_0 \psi_{2L1} - g_{ym} U(t) \psi_{1L2} + \frac{g_{ym}}{2} U(t) \psi_{2L1} = 0, \quad (64)$$

$$i\partial_0 \psi_{2L2} - \frac{g_{ym}}{2} U(t) \psi_{2L2} = 0. \quad (65)$$

As is obvious, the ψ_{1L1} and the ψ_{2L2} are decoupled from each other. If we try to solve for the other wave functions, we get the following solutions: for a general condensate solution of $U(t) = c_1 \text{sn}(g_{ym} c_1 (t + c_2), -1)$,

$$\psi_{1L1}(t) = A_1 \Lambda^{-1/2}, \quad (66)$$

$$\psi_{2L2}(t) = A_2 \Lambda^{-1/2}, \quad (67)$$

$$\psi_{1L2}(t) = c_3 \Lambda^{3/2} + c_4 \Lambda^{-1/2}, \quad (68)$$

$$\psi_{2L1}(t) = -c_3 \Lambda^{3/2} + c_4 \Lambda^{-1/2}, \quad (69)$$

where $\Lambda = (\text{dn}(g_{ym} c_1 (t + c_2), -1) - i \text{cn}(g_{ym} c_1 (t + c_2), -1))$, A_1, A_2, c_3 and c_4 are integration constants, and dn and cn are the Jacobi elliptic functions. Note that even though the condensate seems to couple two different flavours ψ_{1L2}, ψ_{2L1} components, the densities generated by the above solutions are constant.

If we set $\psi_{1L2} = \psi_{2L1}$ in the ODEs as a boundary condition, as that preserves Hamilton's gauge in the "back-reaction", ($j^0 = 0$) then the solution for 1 first order ODE is

$$\psi_{1L2} = \psi_{2L1} = A (\text{dn}(g_{ym} c_1 (t + c_2), -1) - i \text{cn}(g_{ym} c_1 (t + c_2), -1))^{-1/2}, \quad (70)$$

where we have chosen the constant such that the $|\psi_{1L2}|^2 = |A|^2$. However, this choice even though mathematically correct is not physical, as we cannot have current built from a source distribution whose density is zero. If we take $\psi_{1L2} \propto \psi_{2L1}$, of course that allows for a source charge density. In that case, the non-zero current built out of the Fermions are:

$$(j^0)^1 = \psi_{L1}^\dagger \psi_{L2} + \psi_{L2}^\dagger \psi_{L1}, \quad (71)$$

$$(j^0)^2 = -i\psi_{L1}^\dagger \psi_{L2} + i\psi_{L2}^\dagger \psi_{L1}, \quad (72)$$

$$(j^0)^3 = |\psi_{L12}|^2 - |\psi_{L21}|^2. \quad (73)$$

For the space components of the current, we find similar formulas. Putting these in the Yang-Mills equation, we can find the back-reaction of the Fermions on the condensate. What is obvious is that the backreaction breaks the isotropy of the system. One cannot have the condensate as $U(t)\delta_i^a$ as the different internal components $a = 1, 2, 3$ will have different sources. Instead of discussing this further, in this article, we will report on this in a separate publication, which will also discuss the quantum interaction [37].

4.1 In the presence of Gravitational background

In this article, we discuss the quarks + condensate system in the background of a gravitational wave [54, 55]. We find that the interactions connect the modes of a Fermion doublet which allows for ‘flavour’ flip processes. When we solve for the Fermion in the GW background, the solutions are also dependent on the z coordinate. The GW couples to only two of the Fermion wave components.

$$i(\partial_0 + \partial_3)\psi_{2L2} + \frac{g_{ym}}{2}h_+U\psi_{1L1} - \frac{g_{ym}}{2}U\psi_{2L2} = 0, \quad (74)$$

$$i(\partial_0 - \partial_3)\psi_{1L1} + \frac{g_{ym}}{2}h_+U\psi_{2L2} - \frac{g_{ym}}{2}U\psi_{1L1} = 0. \quad (75)$$

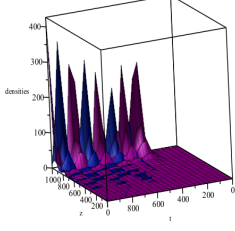
What is obvious is that the two modes in Eqs. (62 & 65), are now interacting, due to the GW. As one can see the GW connects the two Fermions from different elements of the SU(2) doublet. We can solve the coupled equations, and the time evolution of the solutions are plotted in the following graphs. It is evident that the Fermion densities fluctuate in time, due to the GW. The flavour transitions induced by a graviton have been studied in [39]. The evidence for flavour transitions in a GW background obtained in this paper, however, will have relevance for QGP and ‘real’ GW interactions with quarks. GWs have been observed, and at these length scales of 200 MeV, gravity remains classical. Our calculations show that these GW can induce changes in flavour quark fluxes in the presence of a SU(2) condensate. This work might provide interesting insight into the workings of QGP.

The ψ_{2L2} component and ψ_{1L1} component of the Fermion SU(2) doublet in the presence of a GW are plotted in Figs. (18a & 18b). What is obvious is that as the GW couples these otherwise independent modes, there should be a flavour transition induced by the GW. To analyze the flavour flip behaviour, we have plotted the Fermion density without the GW as a function of z to show that the two flavour densities behave differently, one of them increases but the other decreases in the presence of the condensate as expected from the uncoupled behaviour in Fig. (19b). With the GW the density show that there is a coupling effect of the flavours as in Fig. (19d). Similar behavior is observed for the plots in time as in Figs. (19a) & (19c). In the above, we have taken the amplitude of the GW as 1, which is of the same order as the condensate amplitude. This is to solve for the combined effect of the condensate and the GW without one being a perturbation.

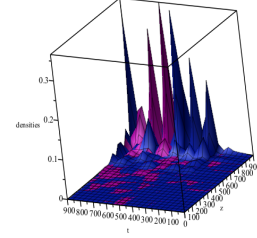
If we try to interpret a perturbation due to a weaker GW, then one takes the Fermion wave functions as $\psi_{2L2} + \tilde{\psi}_{2L2}$ and $\psi_{1L1} + \tilde{\psi}_{1L1}$. The $\tilde{\psi}_{1L1}, \tilde{\psi}_{2L2}$ are perturbations proportional to the GW amplitude, A_+ . The solutions can be obtained using linearized approximations, and the resultant fluxes plotted. It is in this analysis, where the GW is a perturbation over the zeroth order condensate induced quarks/leptons that we find also the phenomena of ‘flip’. We have the following equations, linearized in h_+ :

$$i(\partial_0 + \partial_3)\tilde{\psi}_{2L2} - \frac{g_{ym}}{2}U\tilde{\psi}_{2L2} = -\frac{g_{ym}}{2}h_+U\psi_{1L1}, \quad (76)$$

$$i(\partial_0 - \partial_3)\tilde{\psi}_{1L1} - \frac{g_{ym}}{2}U\tilde{\psi}_{1L1} = -\frac{g_{ym}}{2}h_+U\psi_{2L2}. \quad (77)$$

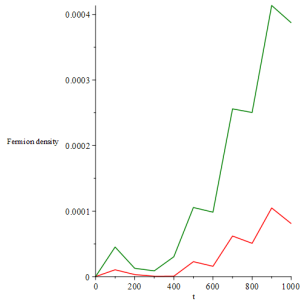


(a) Fermion densities of two flavours with GW at $\omega_g = 10^{-4}$.

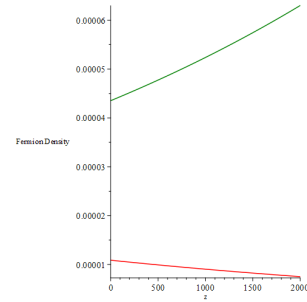


(b) Fermion densities of two different flavours with GW at $\omega_g = 10$.

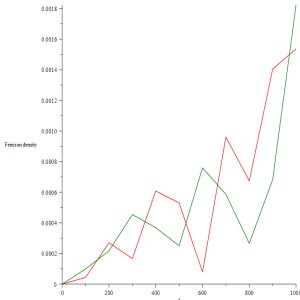
Figure 18: Figures showing Fermion density with a GW for two different flavours.



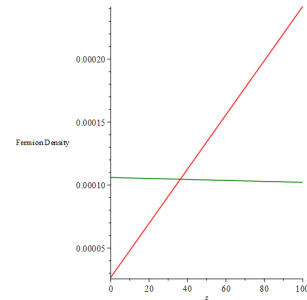
(a) $|\psi_{1L}|^2$ in green and $|\psi_{2L}|^2$ in red without GW as a function of time.



(b) $|\psi_{1L}|^2$ in green and $|\psi_{2L}|^2$ in red without GW as a function of space.



(c) $|\psi_{1L}|^2$ in green and $|\psi_{2L}|^2$ in red with GW as a function of time.



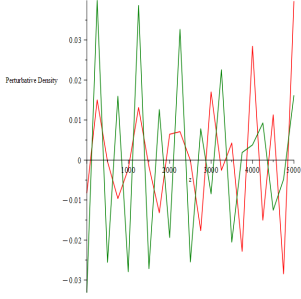
(d) $|\psi_{1L}|^2$ in green and $|\psi_{2L}|^2$ in red with GW as a function of space.

Figure 19: Figures showing Fermion density with and without GW as a function of time and space separately.

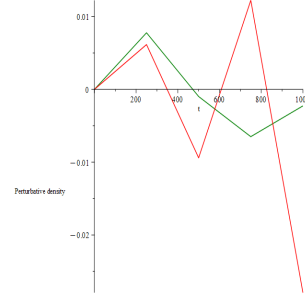
The solutions to the Eqs. (76 & 77) are obtained using numerical methods, and for $g_{ym} = \sqrt{2}$, $c_1 = 1$ and $c_2 = 1/2$, the behaviour of the solutions are shown as graphs. What is interesting here is, however, the perturbation density, which has the form $\psi_{1L1}^* \tilde{\psi}_{1L1}$, $\psi_{2L2}^* \tilde{\psi}_{2L2}$, flip at regular intervals both in space and time. So in other words, if we have u quarks, then interaction with a GW can change the flavour densities, and we would have an enhancement of d quark density. This is because the u quark and the d quark are

‘coupled’ due to the presence of a GW. This phenomenon of flavour switching is shown in Figs. (20a,20b, 20c).

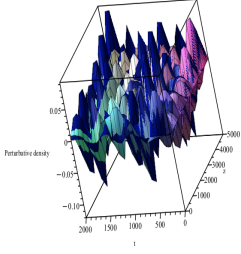
Note that in the above the Fermion density perturbations are allowed to be negative as they enhance or deplete an already existing zeroeth order flux of the two flavours. We have thus isolated the fluctuations in the flavour density induced by the GW, which is of weaker magnitude than the condensate, and that is the scenario in today’s world. If we place the condensate in a SU(3) quark-gluon plasma system, then the GW will induce a transition of the quarks which are coupled by the GW in a SU(2) sub-group. This is an interesting result and can have experimental consequences.



(a) $|\tilde{\psi}_{1L}|^2$ in green and $|\tilde{\psi}_{2L}|^2$ in red plotted in z with $A_+ = 10^{-2}$ and $\omega_g = 1000$.



(b) $|\tilde{\psi}_{1L}|^2$ in green and $|\tilde{\psi}_{2L}|^2$ in red as a function of time with $A_+ = 10^{-2}$ and $\omega_g = 1000$.



(c) $|\tilde{\psi}_{1L}|^2$ and $|\tilde{\psi}_{2L}|^2$ in other colors as a function of space-time with $A_+ = 10^{-2}$ and $\omega_g = 1000$.

Figure 20: Figures showing the $|\tilde{\psi}_{1L}|^2$ and $|\tilde{\psi}_{2L}|^2$.

4.2 Summary:

In this section, we studied the interaction of SU(2) condensate and Fermion SU(2) doublets. At first, we studied how Fermions react in the presence of condensate. There is a mixing of some of the Fermion components. We found that the ψ_{1L1} & ψ_{2L2} (Fermion with flavour 1, Left chirality, component 1; and Fermion with flavour 2, left chirality and component 2) are decoupled and have separate evolution equations (Eqs. (62 & 65)), but, ψ_{1L2} & ψ_{2L1} (Fermion with flavour 1, Left chirality, component 2; and Fermion with flavour 2, left chirality and component 1) are coupled to each other described by two coupled partial differential equations (Eqs. (63 & 64)). When we studied the back-reaction of Fermions on condensate, we found that the back-reaction breaks the isotropy of the YM system. After this, we studied the Fermion + YM condensate system in the presence of a gravitational wave background. We found that there is no change in equations for ψ_{1L2} & ψ_{2L1} , which are still described by Eqs. (63 & 64). But, the ψ_{1L1} & ψ_{2L2} now become coupled by having a dependence on GW as shown in Eqs. (74 & 75). We found that the Fermion densities fluctuate in time exhibiting flavour transitions due to GW. It means if we have two Fermions of the same doublet, the Fermion densities of those flip at regular intervals. This study of Fermion flip is relevant to QGP

and might explain the strangeness of the plasma. In the above computation, we have shown the enhancement of one flavor in the GW-induced interactions with a quark doublet. This can be implemented for a lepton doublet too. If we focus on a QGP in the presence of a GW, the isospin doublets in our discussion for quarks are $(u, d); (c, s)$, and the above show a flux increase of a d quark, or a s quark in presence of a GW. In QFT, precisely these interaction vertices can be used to find heavy flavour generation as in [41] from light quarks. The process of generating heavy flavours (strange) using the GW is work in progress [37].

5 Conclusion

In this article, we have discussed the details of a SU(2) condensate model introduced in [24], in presence of GW and quarks. We also re-analysed the results of energy exchange of the condensate with plasmons. From our re-analysis of the results obtained in [24], we find that their observations that the condensate dissipates into ‘particles’ or ‘plasmons’ is true initially, but the result is highly dependent on the Yang-Mills interaction constant (g_{ym}), and the initial boundary conditions on the plasmons. In our paper, the aim was to study the effect of the GW on the SU(2) condensate. We find that the GW imprints on the condensate generate or induce the plasmons which then decay the condensate. In the gauge invariant ansatz used by [24], we find that the GW interacts only with the symmetric transverse modes identified in their paper. In our re-analysis of the plasmons, the GW interacts with the longitudinal plasmons too. The GW sets the initial boundary conditions on the plasmons, both longitudinal and transverse, and induce the plasmon oscillations. We also find that the decay of condensate energy observed in [24] is delayed compared to the time observed in [24]. The condensate does not decay away all its energy, and the condensate and the plasmons exchange energy in a oscillatory way eventually. This is also shown by the GW+gluon system, which serves to stabilize the plasma. This stabilization of the energy exchange of the plasma-plasmon fields can be used to study the fluid density of the system, and characterize the viscosity of the QGP. It has been shown that the unusually low viscosity of the system can be attributed to the gravitons [38], and our model can be used to verify that hypothesis in presence of GW.

We then introduce quarks in the background of condensate, and we find that quarks break the isotropy of the condensate. This shows that the quarks + gluon system will have to be described by a non-isotropic field, and this sheds light on the nature of the fluid field required to model the QGP. We also solve the quark-condensate system in the background of a GW and find that the GW can induce a flavour transition of the quarks in case the symmetry group is SU(2). One can also interpret this as the transition of quarks transforming in the same SU(2) sub-group in an SU(3) plasma induced by a GW. We find that without the GW, the quark flavour densities remain decoupled, but the GW couples them. In fact, we find that in the example of the u, d flavour doublet, where the d flavour has a lower flux to begin with, the GW causes the d flux to enhance as in Figures (19a,19c,19b,19d). These sorts of ‘flip’ in flavour fluxes can be used to generate strangeness observed in the QGP. In [41], the reactions which give rise to heavy flavour quarks were discussed. Form factors for $q\bar{q} \rightarrow s\bar{s}$ and $gg \rightarrow s\bar{s}$ (q being quark, g being gluons and s being a heavy flavour) were obtained and used in [40] to show enhancement of strangeness. In our calculations, the GW-induced flavour transitions represent interaction vertices which have exactly the same structure as the three particle vertices used in [41]. We therefore expect the contribution of the above interactions to the strangeness generation to be a simple extension. However, we shall be calculating the same process using the GW as an external field instead of a ‘graviton’, and obtaining the enhancement factor [37]. We are also working on resolving the back-reaction and quantum aspects of the quarks of the system in the work in progress [37]. Our calculations will definitely change the ‘strangeness’ enhancement factors discussed in [40] for a QGP formed in the RHIC. In [40], finite temperature versions of the de-confined heavy flavour degeneration is studied. We are currently obtaining the finite temperature distribution functions, and the chemical potentials of the QGP system [37]. In summary, the work we have presented here studies the self-interaction of a gluon condensate, quarks, and how GW induces changes in the ‘plasma’ including flavour

transitions of the quarks. These classical field theoretic calculations have importance for de-confined YM fields, and they provide the basis for a thermodynamic description of QGP found at high temperatures.

Acknowledgement: NRG would like to thank MITACS for accelerator grant.

Declarations: The authors have no competing interests to declare that are relevant to the content of this article. They also declare no conflict of interest with anyone or the funding agencies for conceptualizing and the publication of the results. The authors declare that the results/data/figures have not been published elsewhere, nor are they in consideration for publication by another publisher. The authors declare that the data supporting the findings of this study are available within the paper.

A Appendix: Method of Lines

The basic idea of the Method of Lines (MOL) is to replace the spatial derivatives in the PDE with algebraic approximations using finite difference methods. Then, the spatial derivatives will no longer be a function of spatial variables. Now, the only independent variable that remains in all the functions is time. The PDE is approximated by the system of ODEs in time or a system of Differential Algebraic Equations (DAEs). Now, the problem of solving PDE is reduced to the Initial Value Problem (IVP) of the system of ODEs or DAEs.

Consider a PDE

$$\partial_t \partial_t w(t, x) - \partial_x \partial_x w(t, x) = f(t, x). \quad (78)$$

First, we need to replace the spatial derivative with an algebraic approximation. We can use the centered finite difference method for the first derivative as

$$\partial_x w \approx \frac{w_{i+1} - w_{i-1}}{2\Delta x},$$

where i is an index designating a position along a grid in x and Δx is the spacing in x along the grid. Thus, for the left end value of x , $i = 1$, and the right end value of x , $i = N$ i.e. the grid has N points. Similarly, for the second-order derivative, it is approximated as

$$\partial_x \partial_x w \approx \frac{w_{i+1} - 2w_i + w_{i-1}}{\Delta x^2}.$$

Since the equation is second order in t and x , it requires two initial conditions (ICs) and two boundary conditions (BCs). Let's consider the following ICs and BCs.

$$\begin{aligned} w(t, x = x_i) &= g(t), & \frac{\partial w(t, x = x_f)}{\partial x} &= 0, \\ w(t = 0, x) &= 0, & \frac{\partial w(t = 0, x)}{\partial x} &= 0, \end{aligned}$$

where $g(t)$ is function of time. Using the first BC, we get the value at the first grid point $i = 1$ as

$$w_1(t) = w(t, x = x_i) = g(t), \quad (79)$$

and therefore, we don't need any ODE for $i = 1$.

Substituting the approximating expression for derivatives, the PDE (78) gets transformed as

$$\frac{d^2 w_i}{dt^2} = \frac{w_{i+1} - 2w_i + w_{i-1}}{\Delta x^2} + f(t, x_i), \quad i = 2, 3, \dots, N. \quad (80)$$

For $i = N$, we have

$$\frac{d^2 w_N}{dt^2} = \frac{w_{N+1} - 2w_N + w_{N-1}}{\Delta x^2} + f(t, x_N),$$

but the point w_{N+1} is out of grid. We can sort out this using the second BC. From the secondary BC, using the centered finite difference

$$\partial_x w \approx \frac{w_{N+1} - w_{N-1}}{2\Delta x} = 0,$$

which gives $w_{N+1} = w_{N-1}$. Then, the ODE for $i = N$ is given by

$$\frac{d^2 w_N}{dt^2} = \frac{2w_{N-1} - 2w_N}{\Delta x^2} + f(t, x_N). \quad (81)$$

Finally, we have a DAE system consisting of Eq. (79) for $i = 1$, Eq. (80) for $i = 2, 3, \dots, N-1$ and Eq. (81) for $i = N$. Thus, we have N number of equations for N unknowns ($w_i, i = 1, 2, \dots, N$). This DAE system can be solved using DAE or ODE solvers in Mathematica.

B Appendix: Derivation of the Action in Vector Modes

The Yang-Mills Lagrangian Density is

$$\mathcal{L} = -\frac{1}{4} F_{\mu\nu}^a F^{a\mu\nu}. \quad (82)$$

Using the Hamilton gauge ($A_0^a = 0$), one gets

$$\mathcal{L} = \frac{1}{2} A_i^a \square A_i^a - \frac{1}{2} A_i^a \partial_j \partial_i A^{ja} + g \varepsilon^{abc} A_i^a A_j^b \partial_j A_i^c - \frac{g^2}{4} ((A_i^a A_i^a)^2 - A_i \cdot A_j A_i \cdot A_j).$$

Next, we assume the vector decomposition

$$A_i^a = U(t) \delta_i^a + n_i \Phi^a + \varepsilon_{ilm} n_l s_m^\sigma \chi_\sigma^a. \quad (83)$$

We also assume the following restrictions to get the appropriate splitting of the modes

$$n \cdot \Phi = 0, \quad (84)$$

$$n \cdot \chi_\sigma = 0, \quad (85)$$

$$\varepsilon_{ilm} n_l s_m^\sigma \chi_\sigma^i = 0, \quad (86)$$

This implies that Φ^a has 2 degrees of freedom, and χ_σ^a has 3 degrees of freedom instead of six. Using the above the Lagrangian takes the following form

$$\begin{aligned} \mathcal{L} = & \frac{3}{2} U(t) \square U(t) + \frac{1}{2} \Phi^a \square \Phi^a + \chi_\sigma^a \square \chi_\sigma^a - \frac{1}{2} \Phi^a (n \cdot \partial)^2 \Phi^a - \frac{1}{2} U (n \cdot \partial) (\partial \cdot \Phi) - \frac{1}{2} U \partial_i \partial_a \Lambda_i^a \\ & - \Phi^a (n \cdot \partial) \partial_j \Lambda_j^a - \frac{1}{2} \Lambda_i^a \partial_i \partial_j \Lambda_j^a + g (n \cdot \partial) (s \cdot \chi) U^2 + g \varepsilon^{abc} \chi_\sigma^a \partial^b \chi_\sigma^c U + g \varepsilon^{abc} \chi_\sigma^a \Phi^b (n \cdot \partial) \chi_\sigma^c \\ & + g \varepsilon^{abc} \Lambda_i^a \Lambda_i^b \partial_j \Lambda_j^a - \frac{g^2}{4} (6U^4 + 2U^2 \Phi^2 + 2\Phi^2 \chi^2 + 4U^2 \chi^2 - 4\Phi \cdot \Lambda \cdot \Phi U - 2U^2 \Lambda_j^i \Lambda_j^i \\ & - 2(\Phi \cdot \chi)^2 - 2U^2 \Lambda_j^i \Lambda_j^i - 2U \Lambda_j^i \Lambda_i^a \Lambda_j^a - 2U \Lambda_i^j \Lambda_j^a \Lambda_i^a + \chi^4 - (\chi_i^a \chi_j^a)(\chi_i^a \chi_j^a)), \end{aligned}$$

where we used $\Lambda_j^a = \varepsilon_{ilm} n_l s_m^\sigma \chi_\sigma^a$ for simplification.

To find the Explicit equations of motion (EOM) and assume some form of the fields consistent with the restrictions mentioned above; one takes

$$n = (0, 0, 1), \quad s^1 = (1, 0, 0), \quad s^2 = (0, 1, 0), \quad \Phi^3 = 0, \quad \chi_1^2 = 0, \quad \chi_2^2 = 0. \quad (87)$$

We also assume that the fields are propagating in the longitudinal direction or are functions of (t, z) . This reduces the above Lagrangian to

$$\begin{aligned} \mathcal{L} = & \frac{3}{2}U(-\partial_0^2)U + \frac{1}{2}\Phi^1(-\partial_0^2)\Phi^1 + \frac{1}{2}\Phi^2(-\partial_0^2)\Phi^2 + \frac{1}{2}\chi_1\Box\chi_1 + \frac{1}{2}\chi_2\Box\chi_2 \\ & + gU^2\partial_z(\chi_1 + \chi_2) - \frac{g^2}{4}(6U^4 + 2U^2((\Phi^1)^2 + (\Phi^2)^2) - 4U(\chi_1 - \chi_2)\Phi^1\Phi^2 + 2(\Phi^1)^2\chi_2^2 \\ & + 2(\Phi^2)^2\chi_1^2 + 2U^2(\chi_1 + \chi_2)^2 + 2\chi_1^2\chi_2^2), \end{aligned}$$

where $\chi_1^1 \equiv \chi_1$ and $\chi_2^2 \equiv \chi_2$.

If we add the gravitational wave metric to the Lagrangian (\mathcal{L}), the additional terms (\mathcal{L}_1) generated are proportional to $h^{\mu\nu}$ which is the contravariant gravitational wave fluctuation over the Minkowski metric $\eta^{\mu\nu} - h^{\mu\nu}$, are

$$\mathcal{L}_1 = \frac{1}{4}F_{\mu\nu}^a \left(h^{\mu\lambda} \eta^{\nu\rho} + \eta^{\mu\lambda} h^{\nu\rho} \right) F_{\lambda\rho}^a. \quad (88)$$

In Hamilton's gauge with $A_0^a = 0$ and the Gravitational wave in TT-gauge $h^{11} = h_+ = A_+ \cos(\omega_g(t - z)) = -h^{22}$, one gets

$$\begin{aligned} \mathcal{L}_1 = & -\frac{1}{2}h_+ \left[((\partial_0 A_1^a)(\partial_0 A_1^a) - (\partial_0 A_2^a)(\partial_0 A_2^a)) + \eta^{ij}(\partial_i A_1^a \partial_j A_1^a - \partial_i A_2^a \partial_j A_2^a) \right] \\ & + \frac{g^2 h_+}{4} \left[(A_1 \cdot A_1 - A_2 \cdot A_2) A^2 - \eta^{ij}(A_1 \cdot A_i)(A_1 \cdot A_j) + \eta^{ij}(A_2 \cdot A_i)(A_2 \cdot A_j) \right]. \quad (89) \end{aligned}$$

With the Vector mode decomposition, one gets the additional terms as follows

$$\begin{aligned} \mathcal{L}_1 = & -\frac{1}{2}h_+ [(\partial_0 \chi_1)^2 - (\partial_0 \chi_2)^2] + \frac{g^2}{4}h_+ \left[\chi_2^2 (\Phi^1)^2 - \chi_1^2 (\Phi^2)^2 \right. \\ & \left. + U^2(\chi_2^2 - \chi_1^2) + U^2((\Phi^2)^2 - (\Phi^1)^2) + 2\Phi^1\Phi^2(\chi_1 + \chi_2)U \right] \quad (90) \end{aligned}$$

Then, the total Lagrangian in the presence of GW will be $\mathcal{L} + \mathcal{L}_1$.

References

- [1] T. Schäfer and E. V. Shuryak, "Instantons in qcd", *Rev. Mod. Phys.* **70**, 323–425 (1998).
- [2] V. Gogohia and H. Toki, "Topological structure of a chiral QCD vacuum", *Phys. Rev. D* **61**, 036006, 036006 (2000), [arXiv:hep-ph/9908301](https://arxiv.org/abs/hep-ph/9908301) [hep-ph].
- [3] V. Gogohia and G. Kluge, "Determination of the quantum part of the truly nonperturbative Yang-Mills vacuum energy density in covariant gauge QCD", *Phys. Rev. D* **62**, 076008, 076008 (2000), [arXiv:hep-ph/0002003](https://arxiv.org/abs/hep-ph/0002003) [hep-ph].
- [4] R. Pasechnik and M. Šumbera, "Phenomenological Review on Quark–Gluon Plasma: Concepts vs. Observations", *Universe* **7**, 7, 64 (2017), [arXiv:1611.01533](https://arxiv.org/abs/1611.01533) [hep-ph].

- [5] J.-P. Blaizot, J. Liao, and L. McLerran, “Gluon Transport Equation in the Small Angle Approximation and the Onset of Bose-Einstein Condensation”, *Nucl. Phys. A* **920**, 58–77 (2013), [arXiv:1305.2119 \[hep-ph\]](#).
- [6] J.-P. Blaizot, J. Liao, and L. McLerran, “Gluon Transport Equation in the Small Angle Approximation and the Onset of Bose-Einstein Condensation”, *Nucl. Phys. A* **920**, 58–77 (2013), [arXiv:1305.2119 \[hep-ph\]](#).
- [7] R. C. Hwa and X. N. Wang, *Quark-gluon plasma 4* (2010).
- [8] S. McDonald, S. Jeon, and C. Gale, “3 + 1 D initialization and evolution of the glasma”, *Phys. Rev. C* **108**, 064910, 064910 (2023), [arXiv:2306.04896 \[hep-ph\]](#).
- [9] X.-G. Huang and J. Liao, “Glasma Evolution and Bose-Einstein Condensation with Elastic and Inelastic Collisions”, *Phys. Rev. D* **91**, 116012 (2015), [arXiv:1303.7214 \[nucl-th\]](#).
- [10] E. Elizalde, A. J. Lopez-Revelles, S. D. Odintsov, and S. Y. Vernov, “Cosmological models with Yang-Mills fields”, *Phys. Atom. Nucl.* **76**, 996–1003 (2013), [arXiv:1201.4302 \[hep-th\]](#).
- [11] D. V. Gal’tsov and E. A. Davydov, “Cosmological models with Yang-Mills fields”, *Proc. Steklov Inst. Math.* **272**, 119–140 (2011), [arXiv:1012.2861 \[gr-qc\]](#).
- [12] A. Maleknejad and M. M. Sheikh-Jabbari, “Gauge-flation: Inflation From Non-Abelian Gauge Fields”, *Phys. Lett. B* **723**, 224–228 (2013), [arXiv:1102.1513 \[hep-ph\]](#).
- [13] A. Maleknejad and M. M. Sheikh-Jabbari, “Non-Abelian Gauge Field Inflation”, *Phys. Rev. D* **84**, 043515 (2011), [arXiv:1102.1932 \[hep-ph\]](#).
- [14] F. R. Urban and A. R. Zhitnitsky, “The QCD nature of Dark Energy”, *Nucl. Phys. B* **835**, 135–173 (2010), [arXiv:0909.2684 \[astro-ph.CO\]](#).
- [15] R. Pasechnik, V. Beylin, and G. Vereshkov, “Dark Energy from graviton-mediated interactions in the QCD vacuum”, *JCAP* **06**, 011 (2013), [arXiv:1302.6456 \[gr-qc\]](#).
- [16] R. Pasechnik, G. Prokhorov, and O. Teryaev, “Mirror QCD and Cosmological Constant”, *Universe* **3**, 43, 43 (2017), [arXiv:1609.09249 \[hep-ph\]](#).
- [17] A. Chodos, R. L. Jaffe, K. Johnson, C. B. Thorn, and V. F. Weisskopf, “New extended model of hadrons”, *Phys. Rev. D* **9**, 3471–3495 (1974).
- [18] S. P. Klevansky, “The nambu—jona-lasinio model of quantum chromodynamics”, *Rev. Mod. Phys.* **64**, 649–708 (1992).
- [19] C. Caprini and D. G. Figueroa, “Cosmological backgrounds of gravitational waves”, *Classical and Quantum Gravity* **35**, 163001, 163001 (2018), [arXiv:1801.04268 \[astro-ph.CO\]](#).
- [20] E. Battista and V. De Falco, “First post-Newtonian generation of gravitational waves in Einstein-Cartan theory”, *prd* **104**, 084067, 084067 (2021), [arXiv:2109.01384 \[gr-qc\]](#).
- [21] B. P. Abbott et al., “Observation of gravitational waves from a binary black hole merger”, *Phys. Rev. Lett.* **116**, 061102 (2016).
- [22] P. Saulson, *Fundamentals of interferometric gravitational wave detectors*, G - Reference, Information and Interdisciplinary Subjects Series (World Scientific, 2017).
- [23] N. R. Gosala and A. Dasgupta, “Interaction of Gravitational Waves with Yang-Mills fields”, *to be appear in General Relativity and Gravitation (GRG)*, 10 . 48550 / [arXiv . 2212 . 02416](#) (2022), [arXiv:2212.02416 \[gr-qc\]](#).
- [24] G. Prokhorov, R. Pasechnik, and G. Vereshkov, “Dynamics of wave fluctuations in the homogeneous Yang-Mills condensate”, *JHEP* **07**, 003 (2014), [arXiv:1307.5695 \[hep-th\]](#).

- [25] V. M. Bannur, “Relativistic longitudinal non-Abelian oscillations in quark-antiquark plasma”, *Pramana* **59**, 671–677 (2002).
- [26] J.-P. Blaizot and E. Iancu, “NonAbelian plane waves in the quark - gluon plasma”, *Phys. Lett. B* **326**, 138–144 (1994), [arXiv:hep-ph/9401323](#).
- [27] B. Schenke, “Collective Phenomena in the Non-Equilibrium Quark-Gluon Plasma”, PhD thesis (Frankfurt U., 2008), [arXiv:0810.4306 \[hep-ph\]](#).
- [28] G. Prokhorov, R. Pasechnik, and G. Vereshkov, “Wave fluctuations in the system with some Yang-Mills condensates”, *Physics of Atomic Nuclei* **79**, 1502–1504 (2016).
- [29] F. Fogaca D.S. and Navarra, “Gluon condensates in a cold quark–gluon plasma”, *Phys. Lett. B* **700**, 3, 236 (2011).
- [30] I. A. Batalin, S. G. Matinyan, and G. K. Savvidy, “Vacuum Polarization by a Source-Free Gauge Field”, *Sov. J. Nucl. Phys.* **26**, 214 (1977).
- [31] A. Addazi, A. Marcianò, and R. Pasechnik, “Time-crystal ground state and production of gravitational waves from QCD phase transition”, *Chinese Physics C* **43**, 065101, 065101 (2019), [arXiv:1812.07376 \[hep-th\]](#).
- [32] V. Domcke, Y. Ema, K. Mukaida, and R. Sato, “Chiral anomaly and Schwinger effect in non-abelian gauge theories”, *Journal of High Energy Physics* **2019**, 111, 111 (2019), [arXiv:1812.08021 \[hep-ph\]](#).
- [33] L. Mirzagholi, A. Maleknejad, and K. D. Lozanov, “Production and backreaction of fermions from axion-S U (2) gauge fields during inflation”, *Phys. Rev. D.* **101**, 083528, 083528 (2020), [arXiv:1905.09258 \[hep-th\]](#).
- [34] E. Farhi, J. Goldstone, S. Gutmann, K. Rajagopal, and R. Singleton, “Fermion production in the background of minkowski space classical solutions in spontaneously broken gauge theory”, *Phys. Rev. D* **51**, 4561–4572 (1995).
- [35] P. Adshead and E. I. Sfakianakis, “Fermion production during and after axion inflation”, *Journ. Cosmol. Astr. Phys.* **2015**, 021–021 (2015), [arXiv:1508.00891 \[hep-ph\]](#).
- [36] P. Adshead, L. Pearce, M. Peloso, M. A. Roberts, and L. Sorbo, “Phenomenology of fermion production during axion inflation”, *Journ. Cosmol. Astr. Phys.* **2018**, 020, 020 (2018), [arXiv:1803.04501 \[astro-ph.CO\]](#).
- [37] N. R. Gosala and A. Dasgupta, “Backreaction of fermions on condensate”, preprint (2024).
- [38] Y. Kimura, “Viscosity of quark-gluon plasma and gravitons Bose-Einstein condensate”, arXiv e-prints (2024), [arXiv:2401.16436 \[physics.gen-ph\]](#).
- [39] C. Corianò, L. D. Rose, E. Gabrielli, and L. Trentadue, “Fermion scattering in a gravitational background: electroweak corrections and flavour transitions”, *Journal of High Energy Physics* **2014**, 136, 136 (2014), [arXiv:1312.7657 \[hep-ph\]](#).
- [40] J. Rafelski, “Discovery of Quark-Gluon Plasma: Strangeness Diaries”, *European Physical Journal Special Topics* **229**, 1–140 (2020), [arXiv:1911.00831 \[hep-ph\]](#).
- [41] B. L. Combridge, “Associated Production of Heavy Flavor States in p p and anti-p p Interactions: Some QCD Estimates”, *Nucl. Phys. B* **151**, 429–456 (1979).
- [42] M. E. Peskin and D. V. Schroeder, *An introduction to quantum field theory* (Addison-Wesley, Reading, USA, 1995).
- [43] V. V. Dyadichev, D. V. Gal’tsov, A. G. Zorin, and M. Y. Zotov, “NonAbelian Born-Infeld cosmology”, *Phys. Rev. D* **65**, 084007 (2002), [arXiv:hep-th/0111099](#).

- [44] D. V. Gal'tsov and E. A. Davydov, “Yang-Mills Condensates in Cosmology”, in **International journal of modern physics conference series**, Vol. 14, International Journal of Modern Physics Conference Series (July 2012), pp. 316–325, [arXiv:1112.2943 \[hep-th\]](#).
- [45] D. V. Galtsov and M. S. Volkov, “Yang-Mills cosmology: Cold matter for a hot universe”, **Phys. Lett. B** **256**, 17–21 (1991).
- [46] J. Cembranos, A. Maroto, and S. N. Jareno, “Isotropy theorem for cosmological Yang-Mills theories”, **Phys. Rev. D** **87**, 043523, 043523 (2013), [arXiv:1212.3201 \[astro-ph.CO\]](#).
- [47] W. Magnus and S. Winkler, *Hill's equation. ii: transformations, approximation, examples* (Creative Media Partners, LLC, 2017).
- [48] I. Kovacic, R. Rand, and S. Mohamed Sah, “Mathieu’s Equation and Its Generalizations: Overview of Stability Charts and Their Features”, **Applied Mechanics Reviews** **70**, 020802 (2018).
- [49] I. Kovacic, L. Cveticanin, M. Zukovic, and Z. Rakaric, “Jacobi elliptic functions: a review of nonlinear oscillatory application problems”, **Journal of Sound and Vibration** **380**, 1–36 (2016).
- [50] A. Dasgupta and J. Fajardo-Montenegro, “Aspects of Quantum Gravity Phenomenology and Astrophysics”, **Universe** **9**, 128 (2023), [arXiv:2303.05042 \[gr-qc\]](#).
- [51] R. Allahverdi and A. Mazumdar, “Affleck-Dine condensate, late thermalization, and the gravitino problem”, **Phys. Rev. D** **78**, 043511, 043511 (2008), [arXiv:0802.4430 \[hep-ph\]](#).
- [52] E. Farhi, J. Goldstone, S. Gutmann, K. Rajagopal, and R. Singleton, “Fermion production in the background of minkowski space classical solutions in spontaneously broken gauge theory”, **Phys. Rev. D** **51**, 4561–4572 (1995).
- [53] A. Pich, “The standard model of electroweak interactions”, **Lecture Notes** [arXiv:1201.0537](#), 1–50 (2012).
- [54] N. D. Birrell and P. C. W. Davies, *Quantum Fields in Curved Space*, Cambridge Monographs on Mathematical Physics (Cambridge Univ. Press, Cambridge, UK, Feb. 1984).
- [55] P. Collas and D. Klein, *The dirac equation in curved spacetime: a guide for calculations*, Springer-Briefs in Physics (Springer International Publishing, 2019).